Sufficiency of hypoxia-inducible 2-oxoglutarate dioxygenases to block chemical oxidative stress-induced differentiation of human embryonic stem cells

Sufficiency of hypoxia-inducible 2-oxoglutarate dioxygenases to block chemical oxidative stress-induced differentiation of human embryonic stem cells

Eirini Koutsouraki[1,2], Steve Pells[1,2], Paul A. De Sousa[1,2,†]

[1] Centre for Clinical Brain Sciences, Chancellors Building, 49 Little France Crescent, University of Edinburgh, Edinburgh, EH16 4SB, UK.

[2] MRC Centre for Regenerative Medicine, Scottish Centre for Regenerative Medicine, 5 Little France Dr, Edinburgh, EH16 4UU, UK.

[†]Author for correspondence:
Paul A. De Sousa paul.desousa@ed.ac.uk
Tel: +44-(0)-131-242-6646
Fax: +44-(0)-131-242-6201

Running Title

Dioxygenases in human embryonic stem cells

Graphical Abstract

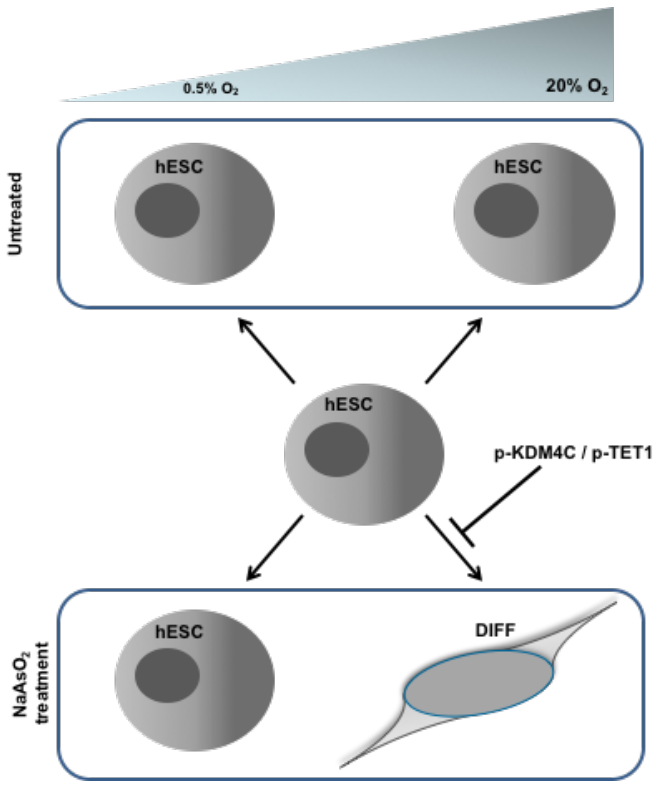

Summary

Hypoxia benefits undifferentiated pluripotent stem cell renewal, and 2-oxoglutarate (2OG) dioxygenases have been implicated in pluripotent stem cell induction and renewal. We show in human embryonic stem cells (hESC) that an ambient oxygen-induced oxidative stress response elicited by culture in a hypoxic atmosphere (0.5% O_2) correlates with the expression of 2OG dioxygenases, which oxidize DNA (TET1, 2, 3) and histone H3 (KDM4C), the former reflected by elevation in genomic 5-hydroxymethylcytosine (5hmC). siRNA-mediated targeting of KDM4C and TET1-3 induces hESC differentiation. Under ambient atmospheric oxygen (21% O_2), exposure to a low inhibitory concentration of sodium arsenite ($NaAsO_2$, IC_{10}), as a model of chemically-induced oxidative stress, suppresses antioxidant gene expression, reduces mitochondrial membrane potential and induces hESC differentiation. Co-administration of the antioxidant N-acetyl-L-cysteine promoted anti-oxidant, pluripotency and 2OG dioxygenase gene expression, elevated genomic hydroxymethylation and blocked induction of differentiation. Transient ectopic expression of KDM4C or TET1 in ambient atmospheric oxygen achieved the same. Our study substantiates a role for 2OG-dependent dioxygenases in hypoxia's promotion of undifferentiated hESC self-renewal.

Highlights

- Hypoxia elevates 2OG-dependent KDM4C and TET mRNAs and genomic 5hmC in hESCs.
- siRNA targeting of KDM4C and TET1-3 induces hESC differentiation.
- In ambient atmospheric conditions, $NaAsO_2$ induces oxidative stress, genomic demethylation and differentiation.
- Co-administration of NAC, Hypoxia, or ectopic expression of KDM4C or TET1 protect against the effects of $NaAsO_2$.

Introduction

Efforts to exploit the potential of human embryonic stem cells (hESCs) and analogous induced pluripotent stem cells (hiPSCs) in regenerative medicine are ongoing. These include their use as source material for cell therapy products such as for the treatment of conditions characterised by acute or chronic cell loss (e.g. macular degeneration, repair of spinal cord trauma, Parkinson's and Huntington's diseases, cardiomyopathy; for up to date accounting go to www.clinicaltrials.gov) and in cell banking initiatives to provide a standardised resource for discovery (e.g. [1]). Such activities necessitate the implementation of best practices in cell culture defined by balance of cost, benefit and risk to efficacy and safety. A case in point is cell cultivation in an ambient atmosphere (21% O_2 in air, commonly referred to as normoxia) vs hypoxic conditions (0.5 to 5% O_2). Despite considerable evidence substantiating the merits of lower oxygen concentrations generally, and in hESC culture specifically (reviewed in [2] and elaborated further below), cultivation under atmospheric oxygen remains common practice. An improved understanding of the mechanisms of hypoxia-mediated benefits is likely to assist in changing practices.

HESC culture in the range of 2-5% O_2, commonly regarded as hypoxic relative to ambient atmosphere but also considered "physiologically normoxic", has broadly been reported to improve undifferentiated colony morphology (e.g. compactness), diminish levels of spontaneous differentiation, increase cell proliferation rate, enhance expression of pluripotency markers, and is associated with a reduced incidence of chromosomal abnormalities ([3-6]). At a molecular level this has been reflected by oxygen-dependent changes in gene expression [7, 8] including i) upregulation of expression of hypoxia-inducible factors at an mRNA or protein level, genes of the glycolytic pathway under their control, the cellular relocalisation and stabilisation of these hypoxia-inducible proteins [5], and also of the c-MYC proto-oncogene [9]; ii) upregulation of substrate attachment mechanisms mediated by specific integrin receptors and CD44 [10]; and iii) activation of Notch signalling [6]. Dioxygenases, specifically the 2-oxoglutarate (2OG)-dependent dioxygenases, are regarded as O_2 sensors that can modulate cellular homeostasis in response to oxidative stress and constitute candidate mediators of ambient oxygen stress-induced epigenetic changes. These include ten-eleven-translocation (TET) enzyme family members (TET1, 2, 3) which oxidise 5-methylcytosine (5mC) to 5-hydroxymethylcytosine (5hmC) and the Jumonji domain 2 (JMJD2)-containing proteins, also known as histone lysine (K)-specific demethylases (e.g. KDM2-7), which oxidise and thereby demethylate specific trimethylated histone residues. All TETs are expressed in mouse and human pluripotent stem cells, and TET1 has been shown to replace OCT4 in the induction of

pluripotency in mouse embryonic fibroblasts [11]. Both the TET1 and KDM4C genes in hESCs are uniquely epigenetically-marked, with distinctive patterns of gene-associated cytosine-guanine island methylation shown to be associated with proper maintenance of a pluripotent phenotype [12]. In mouse ESCs the histone H3-specific demethylase KDM4C has also been shown to act with NANOG in an interconnected regulatory loop, with depletion resulting in differentiation [13]. Genome-wide localisation analyses reveal enrichment of TET1 on regulatory regions marked with H3K4me3 alone or with H3K27me3 [14-16]. Collectively these studies implicate TET1 and KDM4C in the regulation of pluripotency and differentiation.

We sought to investigate the relationship between ambient oxygen, oxidative stress and 2OG dioxygenases in hESC renewal, and the potential of 2OG dioxygenases to mediate the known benefits of hypoxia. Specifically, we assessed; 1) the response of undifferentiated hESCs to culture in a hypoxic (0.5% O_2) vs ambient normoxic (21% O_2) atmosphere at the level of the oxidative stress response, expression of pluripotency genes, KDM4C and TET1-3 expression and genomic methylation and hydroxymethylation; 2) the consequences of RNA interference with expression of KDM4C and TETs; and 3) ambient oxygen dependence of the hESC response to low inhibitory concentrations (IC_{10}) of arsenic in the form of the organic metallic compound sodium arsenite ($NaAsO_2$), a source of chemically-induced oxidative stress [17-21]. Sodium arsenite serves as a model of organometallic contamination of a culture environment, such as could derive from water sources or pressurised atmospheric gas containers. Our findings suggest that hypoxia-induced oxidative stress elevates KDM4C and TET expression, associated with genomic DNA hydroxymethylation, and KDM4C and TETs provide protection against organometallic chemical induction of oxidative stress and cell differentiation.

Results

Our study replicated all experiments in two independent hESC lines to identify conserved outcomes irrespective of known epigenomic (e.g. [12, 22]) and genomic [23] variability between hESC lines. These were the H9 line [24] (main figures) broadly used as a reference standard [23], and the RH1 line derived and utilised by our laboratory [12, 25, 26] (supplementary figures). Conserved outcomes between cell lines are denoted throughout all figures by a solid inverted triangle (▼) with degree of statistical significance noted by asterisks as follows: *p<0.05; **p<0.01; ***p<0.001; ****p<0.0001. In the absence of a solid

inverted triangle symbol, the observed significance pertains only to the cell line depicted in a figure.

Effect of hypoxia on hESC renewal, KDM4C and TET1-3.

HESCs were cultured continuously for 7 days in feeder-free conditions on Matrigel in normoxia (21% O_2 in air) or hypoxia (0.5% O_2), one day after plating in normoxia. Both atmospheres maintained undifferentiated OCT4- and NANOG-positive colonies, although hypoxia significantly increased cell growth over the duration of the experiment (Fig./Suppl. Fig. 1 A-C; $p<0.01$). By ELISA, global genomic 5-hmC increased significantly although this was not qualitatively evident by immunofluorescence microscopy for 5-hmC or mC (Fig./Suppl. Fig. 1 C,D; $p<0.01$). Using RT-qPCR to assess mRNA steady state levels hypoxia increased the relative expression of pluripotency-associated transcription factors (OCT4, NANOG; $p<0.01$), and the 2OG dioxygenases KDM4C, TET1 ($p<0.001$) and TET3 ($p<0.05$) (Fig./Suppl. Fig. 1E). Furthermore, hypoxia significantly increased levels of overall reactive oxygen species (ROS) after days 1 ($p<0.001$) and continuing to day 7 ($p<0.05$) (Fig./Suppl. Fig. 1F). Consistent with this finding was a significant increase in the relative expression of heme oxygenase 1 (HO-1; $p<0.001$), known to be induced by hypoxia [27]. In contrast, there were no differences in the relative expression of antioxidant enzymes (GPX1, GPX4, SOD1, SOD2), or in mitochondrial membrane potential (Fig./Suppl. 1G-H). These findings confirmed prior understanding of the effects of hypoxia on hESC renewal, namely promotion of growth and pluripotency gene expression [3-5]. They also revealed a positive correlation between 2OG dioxygenase expression, genomic hydroxymethylation, ROS and a ROS responsive gene.

Interference with KDM4C and TET1,2,3 in hESCs

Given hypoxia-associated elevation in the expression of KDM4C, TET1 and 3, we next assessed the consequences of interference with these genes. hESC lines were transfected with gene-specific small interfering RNA (siRNA) twice at one day (24 hour) intervals one day after plating, with cells analysed two days after the first transfection (Suppl. Fig. 15). As a negative control to assess general toxicity of the siRNA transfection conditions, cells were transfected with an siRNA (IDS-NULL) composed of randomised sequence derived from the human IDS gene. An siRNA directed against YAP1 was used as an additional control for responses to knockdown of an hESC-expressed gene not required for self-renewal, despite its role in embryonic cell polarisation and ectodermal lineage specification [28, 29]. As a

positive control for an effect on hESC renewal we used an siRNA directed against OCT4. Significant reductions in the steady state level of gene transcripts targeted by each siRNA were confirmed in both cell lines for YAP1, OCT4, KDM4C, TET1 and TET2 ($p<0.05$; Fig./Suppl. Fig. 2A). Interference with OCT4, KDM4C, TETs1-3 individually and TETs1-3 together, but not YAP1 or IDS-NULL, disrupted hESC colony morphology and reduced immunofluorescence for OCT4 and NANOG (Fig./ Suppl. Fig. 2B,C). siRNA targeting of OCT4 consistently reduced relative mRNA levels of NANOG and KDM4C, whereas targeting YAP1 did not, nor did it affect OCT4, TET1, 2 and 3 ($p<0.05$; Fig./Suppl. Fig. 2D). By contrast, interference with KDM4C consistently reduced mRNA levels of KDM4C itself, OCT4, NANOG, TET1 & TET3 ($p<0.01$). Interference with TET1 consistently reduced levels of itself, and KDM4C and increased SOX2 ($p<0.05$). Interference with TET2, TET3 or all three TETs together consistently reduced levels of OCT4 and KDM4C ($p<0.05$) (Fig./Suppl. Fig. 2E).

We next assessed the downstream consequences of RNA interference on genomic methylation by qualitative assessment of 5mC and 5hmC by immunocytochemistry, quantification of the latter by ELISA, and lineage associated gene expression. Interference with IDS-NULL and YAP1 had no effect on genomic 5mC or 5hmC, whereas interference with OCT4 and all of the 2OG dioxygenases qualitatively and quantitatively ($p<0.01$) reduced 5hmC abundance (Fig./Suppl. Fig. 3A,B). To assess whether interference with 2OG dioxygenase RNA resulted in differentiated lineage bias, we defined a germinal lineage marker gene panel consisting of: CDX2, CGα, PL1 (Trophoblast); Brachyury, VEGF, BMP2, GATA2 (Mesoderm); GATA4, AFP, ALBUMIN, HNF4α, GATA6 (Endoderm); PAX6, NESTIN, TUBULIN-III, NF-200 (Ectoderm); and HAND1 (multiple early lineages) (Fig./Suppl. Fig. 3C). Interference with specific 2OG dioxygenases affected specific lineage markers consistently, and differed in which lineage panels were affected. The most compelling evidence of a lineage bias was for ectoderm following knockdown of TET1, as reflected by elevation in all four markers ($p<0.05$). But this was also accompanied by an increase in one mesoderm (BMP2) and two endoderm markers (HNF4α, GATA6), with no effect on trophoblast markers. Otherwise Interference with KDM4C affected genes across all four lineage marker sets, but was confined to an increase in one trophoblast (CGα), one mesoderm (GATA2), two endoderm (GATA4 and GATA6), and one ectoderm (NESTIN) marker ($p<0.05$). Like TET1, knockdown of TET2 affected 3 lineage marker sets, but this time excluding endoderm, and affects were confined to a decrease of one trophoblast marker (CGα) and increase of one mesoderm (BMP2) and one ectoderm marker (PAX6) ($p<0.05$). Inhibition of TET3 affected two lineage marker sets: increasing one mesoderm (BMP2) and one ectoderm (PAX6) marker ($p<0.05$). Concurrent interference with TET1, 2

and 3 affected markers across all four-lineage panels as would be expected, albeit not all of the same genes as when specific TETs were targeted. Again, ectoderm markers were the most affected (elevations in PAX6, TUBULIN III, NF-200), along with an increase in different trophoblast (CDX2) and mesoderm (VEGF, BMP2) markers, a conserved increase in an endoderm marker (GATA6), and an increase in a multiple early lineage marker (HAND1) ($p<0.05$ to $p<0.0001$; Fig./Suppl. Fig. 3C). By comparison, interference with OCT4 affected genes across 3 lineages, this time excluding mesoderm, but was confined to an increase in a trophoblast (CDX2), endoderm (GATA6), and two ectoderm (PAX6 and NESTIN) markers ($p<0.05$).

A role for ambient oxygen in modulating chemically-induced oxidative stress response

Given a positive correlation between hypoxic ambient oxygen, elevation of overall ROS and expression of KDM4C, TET1 and 3 in hESCs, and a role for these genes (and TET2) in maintenance of hESC renewal, we next investigated the consequences of hESC exposure to a low grade chemically-induced oxidative stress under normoxia and hypoxia. To model oxidative stress originating from organometallic contaminants in cell culture-supportive water sources, vessels, materials or gas containers, we established the inhibitory concentration range for hESC lines exposed to arsenic in the form of Sodium Arsenite ($NaAsO_2$) under continuous culture for 7 days under normoxia. $NaAsO_2$ is known to affect cellular redox states, antioxidant defence systems and epigenetic determinants in other cells [18, 29, 30]. Determination of the inhibitory concentration at which we observed a 10% reduction in cell viability (IC_{10}) revealed that this differed widely between lines (H9, $1x10^{-9}$ M; RH1, $3.3x10^{-11}$ M, Suppl. Fig. 12). For both lines, exposure to the cell line-specific IC_{10} consistently resulted in loss of hESC colony morphology, correlated with qualitative loss of OCT4 and NANOG immunofluorescence under normoxia but not hypoxia (Fig./Suppl. Fig. 4A,B). Concurrent treatment with the antioxidant N-acetyl-L-cysteine, NAC, prevented loss of OCT4 and NANOG at normoxia and had no effects under hypoxia (Suppl. Fig. 8A,B). Comparison of mRNA steady state levels under each oxygen atmosphere revealed a consistent and significant ($p<0.0001$) elevation of OCT4, NANOG, SOX2, KDM4C, TET1 and TET2 in $NaAsO_2$-treated cells under hypoxia (relative to untreated), whereas these genes and TET3 were either significantly reduced or unchanged as a result of treatment in normoxia ($p<0.01$; Fig./Suppl. Fig. 4C). Co-administration with NAC significantly elevated OCT4, KDM4C, TET1 and TET3 in normoxia ($p<0.01$), and decreased OCT4, KDM4C and TET2 in hypoxia (Suppl. Fig 9A). $NaAsO_2$ induction of differentiation under normoxia was confirmed by a significant

increase in relative mRNA abundance for BRACHYURY ($p<0.01$; Fig./Suppl. Fig. 4D). This was significantly reduced by co-administration of NAC ($p<0.0001$; Suppl. Fig. 9B). By immunofluorescence microscopy $NaAsO_2$ treatment under normoxia resulted in a loss of 5mC, consistent with previous reports of its inhibition of DNA methyltransferases [30, 31]. This was not evident under hypoxia (Fig./Suppl. Fig. 4B). Co-administration of NAC preserved 5mC fluorescence under normoxia and had no effect on 5mC under hypoxia or 5hmC under normoxia or hypoxia (Suppl. Fig. 8AB). There was no obvious effect of $NaAsO_2$ on 5hmC immunofluorescence in either atmosphere, except for regions of cell differentiation reflected by greater spacing between cells that corresponded with loss of 5mC where it appeared qualitatively brighter under normoxia, (Fig./Suppl. Fig. 4B). As whole mount fluorescence imaging was not confocal we did not attempt to quantify signal intensity as variations could reflect either or both changes in abundance or concentration/diffusion of signal. However, quantification of global 5hmC by ELISA revealed a significant decrease with exposure to $NaAsO_2$ under normoxia ($p<0.001$), but an increase if exposed under hypoxia (Fig./Suppl. Fig. 4E). Hypoxia significantly elevated global 5hmC relative to normoxia in the absence of $NaAsO_2$ as observed previously. Co-administration of NAC with $NaAsO_2$ significantly elevated 5hmC relative to $NaASO_2$ -treated cells under normoxia only ($p<0.0001$;Suppl. Fig. 9C). Thus, the differentiation-inducing effects of $NaAsO_2$ under normoxia could be prevented by antioxidant treatment, which is obviated by hypoxia.

We next assessed ROS in $NaAsO_2$-treated cells under normoxia and hypoxia and included hESCs treated with Buthionine Sulfoximine (BSO), known to elevate ROS (Ji et al., 2010). ROS were significantly elevated in untreated, $NaAsO_2$- and BSO-treated cells under hypoxia relative to normoxia after 1 and 7 days of treatment ($p<0.05$ Fig./Suppl. Fig. 5A). ROS in $NaAsO_2$ and BSO treatment groups were significantly higher than untreated cells in hypoxia after 7 days ($p< 0.001$) and was reduced by co-treatment with NAC (Suppl. Fig. 10A). $NaAsO_2$-induced ROS elevation under hypoxia was matched by a significant increase in the levels of mRNA for hypoxia-inducible HO-1 ($p<0.001$), a measure of oxidative stress, but not the antioxidant genes GPX1, GPX4, SOD1 and SOD2. Levels of the latter four antioxidant transcripts were decreased in both lines treated with $NaAsO_2$ under normoxia only ($p<0.01$; Fig./Suppl. Fig. 5B). Co-administration of NAC significantly elevated HO-1 and the antioxidant genes GPX1 and SOD2 mRNA under normoxia and GPX1 and SOD1 under hypoxia, relative to untreated in each atmosphere (Suppl. Fig. 10B). Under both normoxia and hypoxia treatment with $NaAsO_2$ significantly reduced the mitochondrial membrane potential (MMP) relative to untreated cells ($p<0.001$, Fig./Suppl. Fig. 5C). Addition of NAC improved MMP slightly under both oxygen concentrations although it remained significantly lower in treated vs untreated cells ($p<0.001$; Fig./Suppl. 10C, 11B). Thus, under hypoxia,

protection against $NaAsO_2$-induced differentiation and loss of hydroxymethylation correlates with hypoxia-induced elevation of ROS and HO-1 mRNA levels; however hypoxia does not protect against $NaAsO_2$-induced loss of mitochondrial membrane potential.

A role for KDM4C and TETs in modulating oxidative stress response

To investigate the functional significance of KDM4C and TET1 elevation in hypoxia, and to test if the expression of these alone could protect against the differentiation-inducing effect of $NaAsO_2$ treatment under normoxia, hESC lines were transfected one day after plating with episomal plasmid expression vectors encoding KDM4C (pCXLE-KDM4C), TET1 (pCXLE-TET1), or enhanced Green Fluorescent Protein (pCXLE-eGFP) or no plasmid but exposed to transfection reagent (RNAiMAX Lipofectamine), the latter two conditions serving as negative controls. The transfection efficiency in these experiments was estimated to be 70 % based on transfection with EGFP expressing plasmid (data not shown). This was followed 3 days later by exposure to IC_{10} concentrations of $NaAsO_2$ (or not) for 7 days. In both lines, colony morphology and immunofluorescence for NANOG, and 5hmC were lost by $NaAsO_2$-treated hESCs not transfected with plasmid or transfected with pCXLE-eGFP, whereas transfection with pCXLE-KDM4C or pCXLE-TET1 was protective (Fig. /Suppl. Fig. 6A,B). NaAsO2 induced loss of 5hmC immunofluorescence was not previously observed in earlier experiments, and we speculate that exposure to transfection reagent in these experiments may have facilitated permeability and increasing of effective concentration of NaAsO2 and its consequent effects as has been reported in other cells [32]. Cell transfection with pCXLE-eGFP and post-fixation and permeabilisation in some cells precluded interpretation of microscopic imaging of OCT4 and 5mC immunolabelled with fluorescein in these experiments. RT-qPCR confirmed significant decreases in OCT4, NANOG, SOX2, KDM4C and TET1 in $NaAsO_2$-treated untransfected or pCXLE-eGFP transfected cells which transfection with either 2OG dioxygenase protected against ($p<0.05$; Fig./Suppl. Fig. 6C,D). Quantification of 5hmC by ELISA confirmed significant decreases induced by $NaAsO_2$, and the protective effects of pCXLE-KDM4C and TET1 but not eGFP ($p<0.05$; Fig./Suppl. Fig. 7B,C). Assessment of a limited lineage marker panel consisting of CDX2, BRACHYURY, AFP and PAX6 revealed a conserved increase in CDX2 associated with $NaAsO_2$ treatment alone ($p<0.0001$), or BRACHYURY with p-eGFP transfected $NaAsO_2$ treated cells. However, transfection of $NaAsO_2$-treated cells with pCXLE-KDM4C or pCXLE-TET1 was associated with significantly lower BRACHYURY ($p<0.05$) and unchanged levels of CDX2 and other lineage-associated transcripts (Fig./Suppl. Fig. 7D). Thus, transient expression of either 2OG

dioxygenase alone was sufficient to mimic the protective effect of hypoxia against $NaAsO_2$ induced differentiation.

Discussion

We investigated the possible role for the 2OG dioxygenases KDM4C and TETs as oxygen sensors to mediate the known benefits of hypoxia in support of hESC renewal. We observed that previously reported benefits of hypoxia including promotion of hESC growth and up-regulation of pluripotency-associated transcription factors are accompanied by elevation of ROS, expression of a hypoxia-induced heme-oxygenase, KDM4C and TETs, and global genomic 5hMC. Furthermore, siRNA targeting of KDM4C and TET1-3 induced loss of 5hmC and hESC differentiation. We also observed distinctions between the consequences of hESC exposure to chemically-induced vs hypoxic ambient atmosphere-induced oxidative stress, which involved these dioxygenases. Specifically, under normoxia subcytotoxic exposure to the organometallic compound and known chemical oxidative stressor, $NaAsO_2$, induces loss of 5mC and 5hmC and differentiation, whereas treatment with this compound under hypoxia or ectopic expression of KDM4C or TET1 protects against these effects. Collectively our study substantiates the sufficiency of dioxygenases to protect against chemical oxidative stress-induced differentiation and as a mechanism by which hypoxia promotes pluripotency.

Several studies have confirmed the benefits of lower ambient oxygen concentrations than are present in the atmosphere (21% O_2) for renewal or induction of pluripotency [4, 6, 7, 9, 33, 34] . Oxygen-sensing 2OG dioxygenases such as TET1 and histone lysine-specific demethylases have been implicated in pluripotency renewal [11, 13-16]. However, to our knowledge the sufficiency of 2OG dioxygenases to mediate the benefits of hypoxia in pluripotent stem cells has not been shown. In other cell systems both TET1 and KDM4C have been shown to facilitate/co-activate hypoxia-inducible factor expression, and in turn, to be regulated by them [13, 35-46]. It has also been proposed that the induction of Jumonji domain-containing histone demethylases under low oxygen conditions provides a compensatory mechanism in response to compromised oxygen availability [42]. Our work is consistent with this model and previous studies in other cell types showing that hypoxia induces the transcriptional upregulation of 2OG-dioxygenases KDM4C and TET1. For example, in breast cancer cell lines cultivated in 0.5% O_2, HIF-1 binds to the promoters of dioxygenases generally, and KDM4C specifically, and the expression of these dioxygenases is upregulated. KDM4C specifically catalyses the demethylation of H3K36 [47]. Upregulation

of KDM4C has also been shown previously in hESCs in response to a less hypoxic atmosphere than we used in our study (5% O_2), along with OCT4, NANOG and SOX2 [48]. Hypoxia-induced HIF-1-dependent upregulation of TET1 expression in association with upregulation of canonical hypoxia-responsive genes and genomic 5hmC levels have been demonstrated in neuroblastoma cells [45]. Putative HIF-1α binding sites have been identified in the promoters of TET1 and 3, but not TET2 [15], consistent with our observations of a differential response to hypoxia in the relative abundance of mRNA encoding these proteins.

Our targeted interference with KDM4C and TET1-3 resulted in loss of hESC self-renewal and genome hydroxymethylation in both cell lines for all 2OG dioxygenases. Perturbations in the mRNA steady state level of individual dioxygenases also appeared to affect others differentially. In both lines, we observed that targeting each of KDM4C, TET1 and 3 reduced the level of the others and that these effects were reciprocal. In contrast, targeting TET2 only reduced KDM4C. These results substantiate all of the dioxygenases in our study forming part of the pluripotency gene network. This is further supported by interrogation of the StemCellNet network analysis platform (http://stemcellnet.sysbiolab.eu; [49]), an interactive platform for retrieval and analysis of molecular networks associated with pluripotent stem cells. Based on the studies informing this database, all dioxygenases physically interact or are transcriptionally regulated by a minimum of 3 (TET3) and as many as 26 (KDM4C) stemness associated genes. OCT4, NANOG and SOX2 all directly regulate KDM4C and TET2. OCT4 and NANOG also physically interact with TET1[50]. Further, the transcription factors SMAD2 and 3, downstream of TGF-β/activin type 1 receptor signal transduction, regulate TET1, TET3 and KDM4C (Suppl. Fig. 17).

Assessment of gene interference-induced differentiation using a finite gene marker panel for germinal lineage representation was made difficult by gene marker specific variations, however, interference with TET1 appeared to bias differentiation towards ectoderm in both cell lines. The opposite trend towards mesendoderm differentiation was observed after KDM4C knockdown with the H9 cell line alone. The possibility that this could reflect different lineage potency bias between cell lines cannot be ruled out. However, this was not grossly evident in qualitative in vitro (embryoid body) and in vivo (teratoma) assessments by our group ([25], data not shown). The first report of the consequences of transient silencing of histone-H3 Lysine specific demethylases including KDM4C (JMJD2C) was inconclusive on the nature of differentiation following loss of pluripotency [13]. In mouse ESC clones stably expressing a short-hairpin RNA to TET1, evidence of genomic hydroxymethylation is accompanied by skewing of lineage potential to mesendodermal and extraembryonic lineages, not ectoderm [51]. Mouse gene knockout studies suggest double knockout of TET1

and 2, resulting in complete depletion of genome hydroxymethylation does not result in cell differentiation. Further, although the absence of 5hmC and both TETs induces developmental abnormalities and midgestation and perinatal death, overtly normal development can still occur. [52]. We speculate that divergence of outcomes between our and these studies reflect differences in both experimental method and the response potential of both naïve vs primed states of pluripotency between mouse and human cells, with the comparatively hypomethylated genome in a naïve state defining a lower dependence on 2OG dioxygenase activity to mediate ambient oxygen/reactive oxygen species mediated differentiation induction. Additionally, during development, other compensatory mechanisms exist.

Our study used subcytotoxic exposure to $NaAsO_2$ to achieve a chemically induced oxidative stress. In other cell types, both acute and chronic exposure to $NaAsO_2$ at low concentrations (0.5 - 5μM; still 2-4 fold greater than used here) inhibit DNA methyltransferase enzymes (DNMTs), deplete the S-adenosylmethionine (SAM) pool and result in genomic DNA hypomethylation [31]. At high doses (> 5 μM) it is a general cell poison acting as a sulfhydryl reagent binding to the free thiol groups of enzymes, inhibiting their function and depleting glutathione that destroys cell metabolism. [30, 53]. At low and high doses, reactive oxygen species which it generates induce mitochondrial damage, DNA mutagenesis and apoptosis [17, 19-21]. In vivo, it is a transplacental acting teratogen which interferes with neural development [30]. In vitro studies in mouse embryo stem and carcinoma cell lines report its capacity to inhibit stem cell renewal and embryoid body-mediated or neural stem cell differentiation via suppression of PI3K-AKT and B-catenin and overactivation of MEK-ERK signal transduction pathways [54-56]. ERK activation is necessary for mesoderm differentiation, and reactive oxygen species enhance differentiation into the mesendodermal lineage[57-59]. Although our study did not attempt to characterise differentiation induced by $NaAsO_2$ under normoxia, elevation of the mesodermal marker Brachyury aligns with these findings.

Supplementation of culture media with substances with antioxidant activity (e.g. NAC, or more commonly ß-mercaptoethanol, dithiothreitol, glutathione, lipoic acid, or Vitamins [C, E]) is a standard approach to counter ROS production in culture. But, the presence of these in the media systems used in these experiments were still insufficient to counter ROS produced by subcytotoxic $NaAsO_2$ exposure. For this, the hypoxia induced molecular responses, evidenced in our study by elevation of HO-1 expression, are necessary, or more specifically the elevation of 2OG dioxygenase expression downstream of this response, as we demonstrate. Hypoxia's ability to block $NaAsO_2$ induction of differentiation occurred

despite its own induction of ROS, and further reduction of mitochondrial membrane potential. Our study intentionally utilised a generic fluorescence-based ROS reporter (2', 7'-dichlorofluorescein diacetate; DCF-DA) in the first instance which as a consequence precluded discrimination of the origin of reactive oxygen species (i.e. O_2^-, $OH^\bullet$, $NO_2^\bullet$ and $ONOO^-$). This requires investigation in future studies. Both hypoxia and $NaAsO_2$ are likely to elicit ROS by different mechanisms, with our study observing a difference at the level of HO-1 induction at least at the single time points assessed. Our study used low inhibitory IC_{10} exposures (empirically determined for each cell line) as a model for chemical contamination which could derive from water or vessels used in tissue culture. Importantly, these IC_{10} values were at least 2-4 orders of magnitude lower than World Health Organisation Guidelines for naturally-occurring chemicals that are of health significance in drinking water (10 parts per billion, for $NaAsO_2$, equating to 0.77×10^{-7} M; WHO, 2011). Water quality in cell culture has long been understood to be an important issue, yet certificates of analyses that accompany commercially-supplied media do not normally qualify chemical contaminant levels. To our knowledge there have been no published investigations of arsenic as a contaminant in routine cell culture materials or vessels. It is interesting to ponder the extent to which variation encountered in the ability to maintain undifferentiated pluripotent stem cells across cell lines in different laboratories and with different reagents might be affected by subcytotoxic contamination of cultures with organometallic compounds such as arsenic. We suggest in the light of our data that an additional benefit of culturing pluripotent stem cells in hypoxic atmosphere is protection against such influences and furthermore, that the certification of reagents for pluripotent stem cell culture should include levels of trace organometallic compounds.

In conclusion, our study furthers understanding of the known benefits of hypoxia to promote undifferentiated pluripotent hESC growth by demonstrating a role for oxygen-sensing dioxygenases, specifically KDM4C and TET1, which alone can protect against differentiation induced by chemical oxidative stress. This supports implementation of hypoxia as best practice in the culture of human pluripotent cells.

Experimental Procedures

Cell culture of hESCs

Experiments were performed on RH1 [25] and H9 [24] hESC lines derived from cryopreserved stocks cultured under feeder-free conditions, in a human dermal fibroblast-

conditioned medium supplemented with 4 ng/ml of human basic fibroblast growth factor (Peprotech), nutrients and 20% Knockout serum replacement (HDF-CM+). Cells were plated on Matrigel (BD Biosciences)-coated plates under a humidified atmosphere of 5% CO_2 in air (21% O_2) at 37°C, as described previously [25]. Unless otherwise stated, experiments were performed on cell lines transitioned for at least 5 passages into mTeSR1 (StemCell Technologies) on Matrigel, and used within a recorded feeder-free passage number range between p45 and 70. For hypoxic induction, hESCs were cultured in a multi-gas incubator where nitrogen gas was supplied to maintain the controlled reduced percentage of 0.5% O_2. For hypoxic cultures, cell culture media and PBS were all incubated in the hypoxic atmosphere overnight prior to every medium change in order to minimize the exposure of cells to atmospheric oxygen levels (21% O_2). Medium changes were performed every two days and the process was performed within two minutes in order to reduce exposure to atmospheric oxygen as much as possible, unless otherwise stated. For each ambient atmosphere hESC lines were seeded in triplicate cultures for each time point to be harvested, in a 6-well plate format (20,000 per cm^2). Cells were harvested at each time point for cell counting. Cell numbers were determined using a haemocytometer to count 0.01% Trypsin-EDTA- passaged single cell suspensions.

Subcytotoxic treatment of compounds on undifferentiated hESCs

$NaAsO_2$ concentration treatment cytotoxic range finding for each cell line was performed first using undifferentiated hESCs cultured with HDF-CM+ culture medium. At day 0, hESCs were seeded in triplicate cultures for each concentration at a density of $1x10^4$ cells/well in 96-well tissue culture plates in 0.1 ml of HDF-CM+ medium and then cultivated for 24 hours at 5% CO_2 in humidified air at 37°C. The following day, the culture medium was withdrawn and replaced with medium containing a specified concentration of $NaAsO_2$. Over 7 days of treatment, cultivation media were refreshed every 48 hours. At the endpoint of culture viable cell numbers were assessed with the CellTiter-Blue Cell Viability Assay (Promega) according to manufacturer's instructions with each well being measured at 560 nm using a POLARstar Optima microplate reader (BMG LABTECH). Cytotoxic range profiles for each cell line were independently confirmed in feeder-free mTESR-1/Matrigel culture conditions (data not shown). For experiments evaluating $NaAsO_2$ at line-specific IC_{10} treatment concentrations, hESC lines were seeded at $5x10^4$ cells/well in HDF-CM+/Matrigel-coated 12-well plates for 24 hours prior to treatment. Treatments were for 7 days with media refreshed every two days as for cytotoxicity range finder experiments.

Determination of reactive oxygen species (ROS) production

The generation of ROS in hESC cultures was evaluated using the fluorescent dye 2', 7'-dichlorofluorescein diacetate (DCF-DA; 2 μM). Briefly, hESC were seeded in 6-well Matrigel-coated plates and exposed to a normoxia/hypoxia atmosphere with or without $NaAsO_2$ for one or seven days. Harvested cells were DCF-DA treated (control + dye) or not (control – dye) in PBS for 40 min in a 37°C water bath in darkness. Following incubation, the fluorescence was measured using a FACSCalibur (BD Biosciences) flow cytometer. The brightness of the fluorescence is considered to reflect the extent to which ROS are present [60, 61]. Fluorescence intensity of at least $1x10^4$ cells was measured for each sample and experiments performed in quadruplicate. Data were analysed using the FCS Express 4 Image Cytometry software (De Novo Software).

Determination of mitochondrial membrane potential (MMP)

The mitochondrial membrane potential in hESCs was measured using Rhodamine 123. Briefly, cells were cultured in 96-well plates and treated with $NaAsO_2$ under normoxic (21% O_2) and hypoxic (0.5% O_2) atmospheres for seven days. At day 7, cells were washed once with PBS and incubated with Rhodamine 123 (2 μM) for 40 min at 37°C in darkness. Following incubation, the fluorescence was quantified using a POLARstar Optima microplate reader. The fluorescence intensity was measured for quadruplicate biological samples and experiments performed in triplicate for each human ESC line.

RNA isolation, reverse transcription and quantitative real-time PCR analysis

Total RNA isolation was performed using TRIzol Reagent (Life Technologies), according to the manufacturer's protocol. CDNA was synthesized using the SuperScript III First-Strand Synthesis System for RT-PCR Kit (ThermoFisher Scientific) according to the manufacturer's instructions using oligo(dT) primers. Quantitative RT-PCR (RT-qPCR) for each gene transcript in each biological replicate was executed in triplicate using the DyNAmo Flash SYBR Green qPCR Kit (ThermoFisher Scientific) and reactions were amplified with a StepOne Plus thermocycler (Applied Biosystems). A standard thermocycling protocol was applied for all genes consisting of: 1) initial denaturation for 7 min at 95°C; 2) Denaturation

for 10 sec at 95°C; 3) Annealing/extension for 30 sec at 58-60°C; 4) 40 cycles of steps 2 and 3; and 5) a melting curve lasting 25 sec over a temperature range of 65 to 95°C. Triplicate reactions were assessed to determine the cycle threshold (Ct) value for a given transcript. If data from the parallel reactions varied more than 0.5 cycles, the reactions were repeated or excluded from the data analysis. The Ct values of the target genes were normalised against those of the housekeeping genes GAPDH or β-ACTIN, depending on experimental conditions. GAPDH was used in siRNA experiments and β-ACTIN in all experiments where atmospheric oxygen was a variable experimental parameter given the oxygen dependence of the former. In the event of comparison of outcomes between atmospheric atmospheres, results are expressed as fold change relative to normoxia. Oligonucleotide primer sequences are tabulated in Suppl. Fig.14, and reported previously [12, 62, 63].

Immunocytochemistry

Indirect immunofluorescence for OCT4, NANOG, 5mC and 5hmC were performed as previously described in and references therein. Primary and secondary antibody suppliers and dilutions are provided in Suppl. Fig. 13. Nuclei were labelled with DAPI. Images were captured using a Zeiss Observer fluorescence microscope and prepared using Zeiss AxioVision 4.8.2 software.

Enzyme-linked immunosorbent assay (ELISA) of global DNA 5hmC content

The 5hmC content of extracted genomic DNA from untreated and treated hESCs was measured using a hydroxymethylated DNA quantification kit (Quest 5hmC DNA ELISA Kit, ZYMO Research) according to manufacturer's protocol. The quantification of the 5-hmC was performed by reading the absorbance at 450 nm in a POLARstar OPTIMA microplate reader. The percentage of 5hmC in samples was calculated based on a standard curve generated according to the manufacturer's instructions. A minimum of quadruplicate biological replicates were run unless indicated otherwise.

Small Interfering RNA (siRNA) knockdown

Quadruplicate cultures of hESCs in mTESR-1 on Matrigel were transfected with target-specific siRNA twice at 24 hours intervals, 48 hours and 72 hours after plating (Suppl. Fig. 15). Targeted genes included KDM4C, TET1, TET2, TET3, all 3 TETs concurrently, OCT4

and YAP1 (reference genes required and not required for hESC renewal, respectively [12, 64]). As a further control for non-specific effects of siRNA transfection, hESCs also were transfected with a mutated sequence based on the human IDS gene (IDS-NULL) which targets no sequence in the human genome, against which effects on gene expression could also be normalised. To assess targeted siRNA effects on gene expression, transcript-specific mRNA first normalised internally to GAPDH values for each siRNA treated cell sample, were then calculated as fold differences relative to IDS-NULL-treated samples. siRNAs were transfected into hESCs using RNAiMAX Lipofectamine (Invitrogen) according to manufacturer's instructions. SiRNA sequences target specificity was checked using SpliceCenter [65]. Gene targeted siRNA sequences were as follows: IDS-NULL, GGCGACACCACCUAACAUU; YAP1, UCACAUCGAUCAGACAACA; OCT4, AUCUUCAGGAGAUAUGCAA; KDM4C, GUACAUCUGUAACAGAAGA; TET1, ACUCUGAAGUUGACAAG; TET2, CAAGACCAAUGUCAGAA; TET3, GAUGAAGGUCCAUAUUA. Cells were harvested for analysis 24 hrs after the second siRNA transfection.

Nucleofection of hESCs with expression plasmids

HESCs were harvested by trypsinization. They were then transfected with episomal plasmids by nucleofection of $4x10^5$ cells with 0.29 µg DNA in a 20 µl reaction using nucleofection solution P2 and program EN-150 and running on a 4D-Nucleofector system (Lonza). Following transfection, cells were quickly transferred into Matrigel -coated 6-well plates containing pre-warmed mTeSR1 medium. Episomal plasmids and their preparation for nucleofection were as reported previously ([12]; Suppl. Fig.16).

Statistical analysis

Statistical analyses were performed using GraphPad Prism software version 5 for Windows (GraphPad Software, San Diego, California USA). Values are expressed as the mean ± standard deviation (SD) throughout. Differences between the various conditions were assessed by unpaired t-test or one-way ANOVA with Dunnett's post-test, as appropriate, unless otherwise specified.

StemCelNet Network Analysis

To identify prospective molecular interactions between dioxygenases in our study with pluripotency and non-pluripotency associated genes we interrogated *StemCellNet (http://stemcellnet.sysbiolab.eu; [49]*). The StemCellNet database includes i) 11 independently published mouse and human embryonic stem cell gene expression studies; ii) , physical protein interactions in murine embryonic stem cells identified using affinity purification and mass spectrometry to identify targets in seven studies whose targets included pluripotency associated transcription factors (ie. example OCT4-POU5F1, NANOG, SOX2); iii) transcriptional regulatory interactions by chromatin immunoprecipitation combined with microarray and sequencing technologies in 18 studies targeting the pluripotency associated transcription factors; iv) physical and regulatory interactions from the Unified Human interactome data. The last incorporates data from 15 primary sources (MDC-Y2H, CCSB, HPRD, BioGRID, BIND, DIP, IntACT, Reactome, COCIT, ORTHO, HOMOMINT, OPHID, TRANSFAC-public version, miRTarBase, HRRIdb). The StemCellNet database defines stemness gene sets from i-iii) of the aforementioned resources and scale functional RNAi screens to detect genes whose knock-down leads to loss of stem cell markers.

Acknowledgments

The authors thank Kay Samuel for initial technical help with flow cytometry and Prof. Agapios Sacchinidis for germinal lineage marker RT-qPCR primer sequences. This project was supported by EUFP7 funding to P A De Sousa as part of the ESNATS (Embryonic Stem Cell Novel Alternative Testing Strategies) consortium (FP7-201619).

Authors contributions

EK, conceived and performed experiments, did initial statistical analysis and interpretation of data, and prepared first draft of manuscript and figures; SP, prepared the KDM4C and TET1 plasmids and edited the manuscript; PADS, secured funding, supervised experimental design, performance, data analysis and interpretation, and led drafting of manuscript revision, submission and responses to reviews.

Disclosure of Potential Conflicts of Interest

The authors declare no competing financial interests.

Figure Legends

Figure 1. Effect of hypoxia versus normoxia on measures of hESC phenotype, dioxygenase expression and function and oxidative stress as assessed in H9 hESCs. **(A)** Compacted colony morphologies observed following 7 days of feeder-free cultivation under normoxia (21% O_2) vs hypoxia (0.5% O_2). Bar equals 100 µm. **(B)** Hypoxia enhances hESC growth over 7 days of cultivation. Bars depict the mean fold increase from day of seeding ± SD to each time for each atmosphere (Seeding Density 20,000/cm^2; n=3). **(C)** Representative immunocytochemical detection of OCT4, NANOG, 5mC, 5hmC and fluorescent staining of nuclear DNA (DAPI) after 7 days of culture. Bar equals 100 µm. **(D)** ELISA quantification of 5hmC after 7 days of culture. Bar depicts mean ± SD (n=3). **(E)** Log_{10} fold change in steady state level of mRNA for pluripotency genes (OCT4, NANOG and SOX2) and dioxygenases (KDM4C, TET1, TET2 and TET3) after 7 days in hypoxia relative to normoxia, set as 1 (n=4) **(F)** Generation of ROS at days 1 (D1) and 7 (D7) of culture under normoxia vs hypoxia assessed by flow cytometry detection of DCF dye fluorescence emission from stained (CTRL + dye) and unstained cells (CTRL - dye). Bars depict mean values ± SD of n= 6 (D1) and 7 (D7). **(G)** Hypoxia elevates steady state level of mRNA for HO-1 but not GPX1, GPX4, SOD1 and SOD2 assessed at 7 days of culture. Log_{10} fold increase in hypoxia treated cells relative to normoxia, set as 1 (n=4). **(H)** Mitochondrial membrane potential did not vary between cells cultured under both atmospheres for 7 days, as assessed by Rhodamine 123 fluorescence intensity. Bars represent mean fluorescence intensity ± SD (n=3). Conserved outcomes between cell lines (▼). Asterisks denote level of significance for representative outcomes for H9 (*p<0.05; **p<0.01; ***p<0.001; ****p<0.0001).

Figure 2. RNA interference targeting OCT4, KDM4C and TET1/2/3 perturbs morphological and molecular measures of pluripotency as assessed in H9 hESCs. (A) Log_{10} fold change in steady state mRNA level of the siRNA targeted genes (YAP1, OCT4, KDM4C, TET1, TET2, TET3 and TET1-3 concurrently) expressed relative to cells transfected with random sequence derived from human IDS gene (IDS-NULL) (n=4). **(B)** Representative colony morphology corresponding to aforementioned siRNA transfections. Transfection with YAP1 and IDS-NULL siRNA have no effect on colony morphology, whereas targeting of OCT4, KDM4C and TET1-3 does. Bar equals 100 µm. **(C)** Immunocytochemistry for OCT4 and NANOG corresponding to aforementioned transfections. Transfection with YAP1 and IDS-NULL siRNA have no qualitative effect on immunostaining for pluripotency markers whereas targeting of OCT4, KDM4C, TET1-3 does. Bar equals 100 µm. **(D)** Log_{10} fold change in state levels of mRNAs for pluripotency associated transcription factors (OCT4, NANOG, SOX2) and dioxygenases (KDM4C, TET1,2,3 and TET1-3 inclusive) following siRNA targeting of YAP1 and OCT4 as above (n=4). Only targeting OCT4 results in significant changes in pluripotency or dioxygenase gene transcription. **(E)** Log_{10} fold change in state levels of mRNAs for pluripotency associated transcription factors (OCT4, NANOG, SOX2) and dioxygenases (KDM4C, TET1,2,3 and TET1-3) following siRNA targeting of dioxygenases (n=4). Consistent with effects on morphology and OCT4 and NANOG immunocytochemistry, targeting all dioxygenases generally results in significant lowering of OCT4, NANOG and other dioxygenases. Conserved outcomes between cell lines (▼). Asterisks denote level of significance for representative outcomes for H9 (*p<0.05; **p<0.01; ***p<0.001; ****p<0.0001).

Figure 3. RNA interference targeting KDM4C and TET1/2/3 in H9 hESCs lowers genomic 5hmC content and induces differentiation associated alterations in lineage marker expression. (A) Representative immunocytochemical detection of 5mC and 5hmC and fluorescent labelling of nuclear DNA (DAPI) following transfection with siRNAs directed against IDS-NULL, YAP1, OCT4, KDM4C, TET1, TET2, TET3 and TET1-3. Bar equals 100 µm. **(B)** ELISA quantification of 5hmC in siRNA treated cells. Bars represent mean percentage of genomic DNA +/- SD (n=3). **(C)** Log_{10} fold change after siRNA treatments expressed relative to cells transfected with random sequence derived from human IDS gene (IDS-NULL), set as 1 (n=4). Conserved outcomes between cell lines (▼). Asterisks denote level of significance for representative outcomes for H9 (*p<0.05; **p<0.01; ***p<0.001; ****p<0.0001).

Figure 4. Differential effects of $NaAsO_2$ under normoxia vs hypoxia on measures of hESC phenotype and dioxygenase expression and function as assessed in H9 hESCs. **(A)** $NaAsO_2$ disrupts undifferentiated colony morphology under normoxia but not hypoxia. Bar equals 100 μm. **(B)** Representative immunofluorescent staining for OCT4, NANOG, 5mC, 5hmC and nuclear DNA (DAPI) following treatment with $NaAsO_2$ or not under normoxia or hypoxia. Bar equals 100 μm. **(C)** Log_{10} fold change in levels of mRNA for OCT4, NANOG, SOX2, KDM4C, TET1, TET2 and TET3 following treatment with $NaAsO_2$ under normoxia or hypoxia expressed relative to untreated cells in the same atmosphere, set as 1 (n=4). **(D)** Log_{10} fold change in levels of mRNA for germinal lineage markers CDX2, BRACHYURY, AFP and PAX6 under normoxia following treatment with $NaAsO_2$ expressed relative to untreated cells set as 1 (n=4). **(E)** ELISA quantification of 5-hmC in $NaAsO_2$ treated and untreated cells in normoxia vs hypoxia. Bars equal mean $\pm$ SD (n=3). Conserved outcomes between cell lines (▼). Asterisks denote level of significance for representative outcomes for H9 (*p<0.05; **p<0.01; ***p<0.001; ****p<0.0001).

Figure 5. Differential effects of $NaAsO_2$ under normoxia vs hypoxia evident in measures of oxidative stress as assessed in H9 hESCs. (A) Generation of ROS at days 1 (D1) and 7 (D7) of culture following treatment or not with $NaAsO_2$ under normoxia vs hypoxia. ROS were determined by flow cytometry detection of DCF dye fluorescence emission from stained (CTRL + dye) and unstained cells (CTRL - dye) cells. Buthionine Sulfoximine (BSO) is known to elevate ROS. Bars depict mean values $\pm$ SD of n= 6 (D1) and 7 (D7). **(B)** Log_{10} fold change in levels of mRNA for HO-1 and antioxidants GPX1, GPX4, SOD1, SOD2 in $NaAsO_2$ treated cells under normoxia vs hypoxia expressed relative to untreated cells, set as 1 (n=4). **(C)** Mitochondrial membrane potential in $NaAsO_2$ treated and untreated control cells under normoxia or hypoxia. Bars represent mean Rhodamine 123 fluorescence intensity $\pm$ SD (n=4). Conserved outcomes between cell lines (▼). Asterisks denote level of significance for representative outcomes for H9 (*p<0.05; **p<0.01; ***p<0.001; ****p<0.0001).

Figure 6. Transfection with plasmids encoding KDM4C or TET1 protects against $NaAsO_2$ induced differentiation under normoxia as assessed in H9 hESCs. (A) Compacted colony morphology is protected by transfection with plasmids (pCXLE-) encoding KDM4C and TET1 but not eGFP, or exposed to transfection reagents only prior to treatment with $NaAsO_2$ under normoxia. Bar equals 100 µm. **(B)** Immunofluorescent staining for OCT4 and NANOG correlate with aforementioned effects on colony morphology. Bar equals 100 µm. Corresponding cell nuclei depicted by DAPI staining. **(C)** Log_{10} fold change in mRNA for OCT4, NANOG, SOX2 in aforementioned treatment groups depicted relative to untreated control (no plasmid) set as 1 (n=4). **(D)** Log_{10} fold change in mRNA for KDM4C, TET1, TET2 and TET3 in aforementioned treatment groups. Gene transcript levels are internally normalised to GAPDH and depicted relative to untreated control (no plasmid) set as 1 (n=4). Conserved outcomes between cell lines (▼). Asterisks denote level of significance for representative outcomes for H9 (*p<0.05; **p<0.01; ***p<0.001; ****p<0.0001).

Figure 7. Transfection with plasmids encoding KDM4C or TET1 promotes genomic 5hmC content and inhibits differentiated lineage marker expression despite treatment with $NaAsO_2$ under normoxia as assessed in H9 hESCs. (A) Immunofluorescent staining for 5mC and 5hmC correlate with aforementioned effects on colony morphology. Bar equals 100 µm. Corresponding cell nuclei depicted by DAPI staining. **(B)** ELISA quantification of 5hmC in pCXLE-KDM4C transfection experiment. Bars represent mean ± SD (n=3). **(C)** ELISA quantification of 5-hmC in pCXLE-TET1 transfection experiment. Bars represent mean ± SD (n=3). **(D)** Log_{10} fold change in mRNA for CDX2, BRACHYURY, AFP, and PAX6 following transfection of pCXLE-eGFP, KDM4C, and TET1, or no plasmid (transfection reagents) and treatment with $NaAsO_2$ depicted relative to untreated (and no plasmid) control set as 1 (n=4). Conserved outcomes between cell lines (▼). Asterisks denote level of significance for representative outcomes for H9 (*p<0.05; **p<0.01; ***p<0.001; ****p<0.0001).

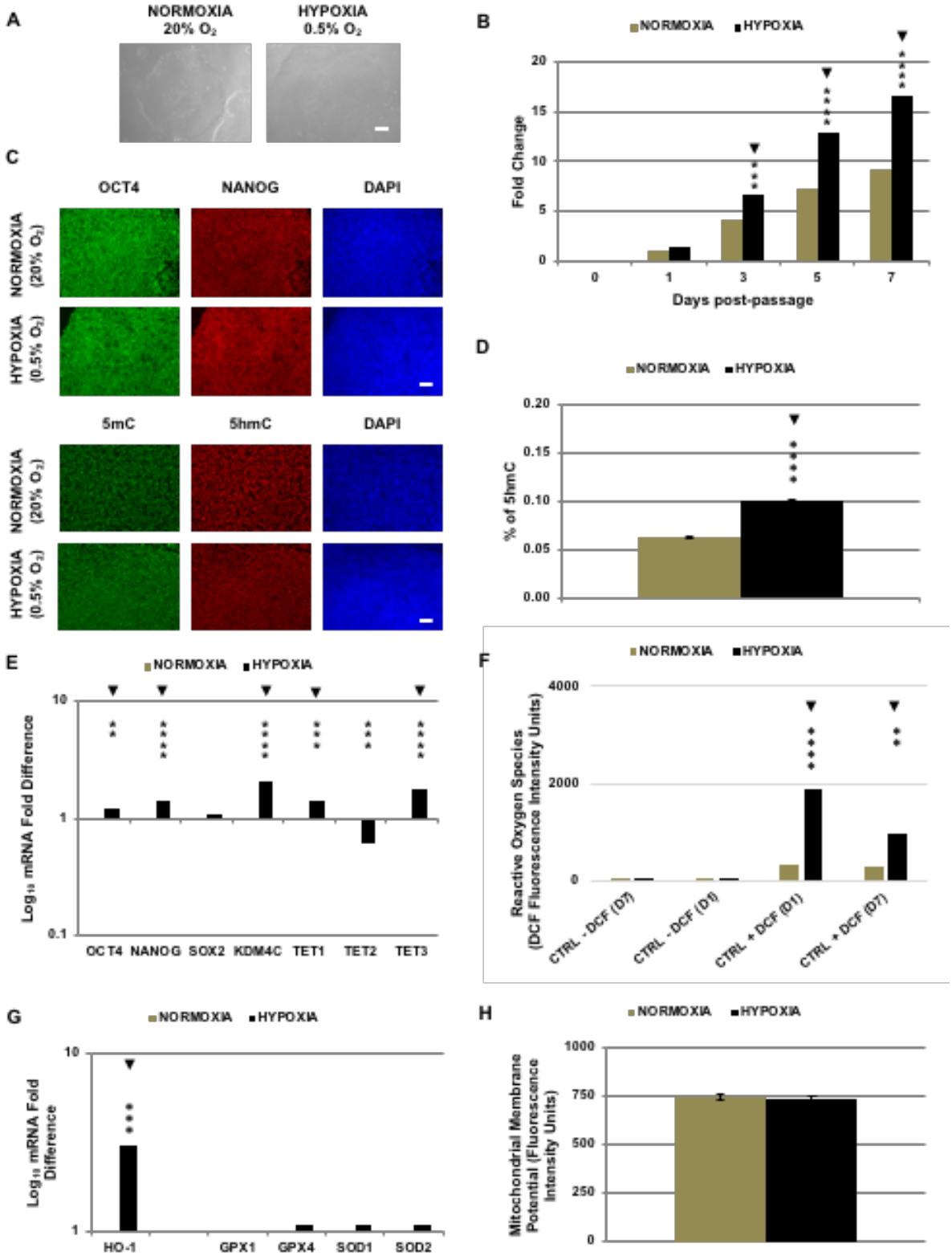

Figure 1. Effect of hypoxia versus normoxia on measures of hESC phenotype, dioxygenase expression and function and oxidative stress as assessed in H9 hESC.

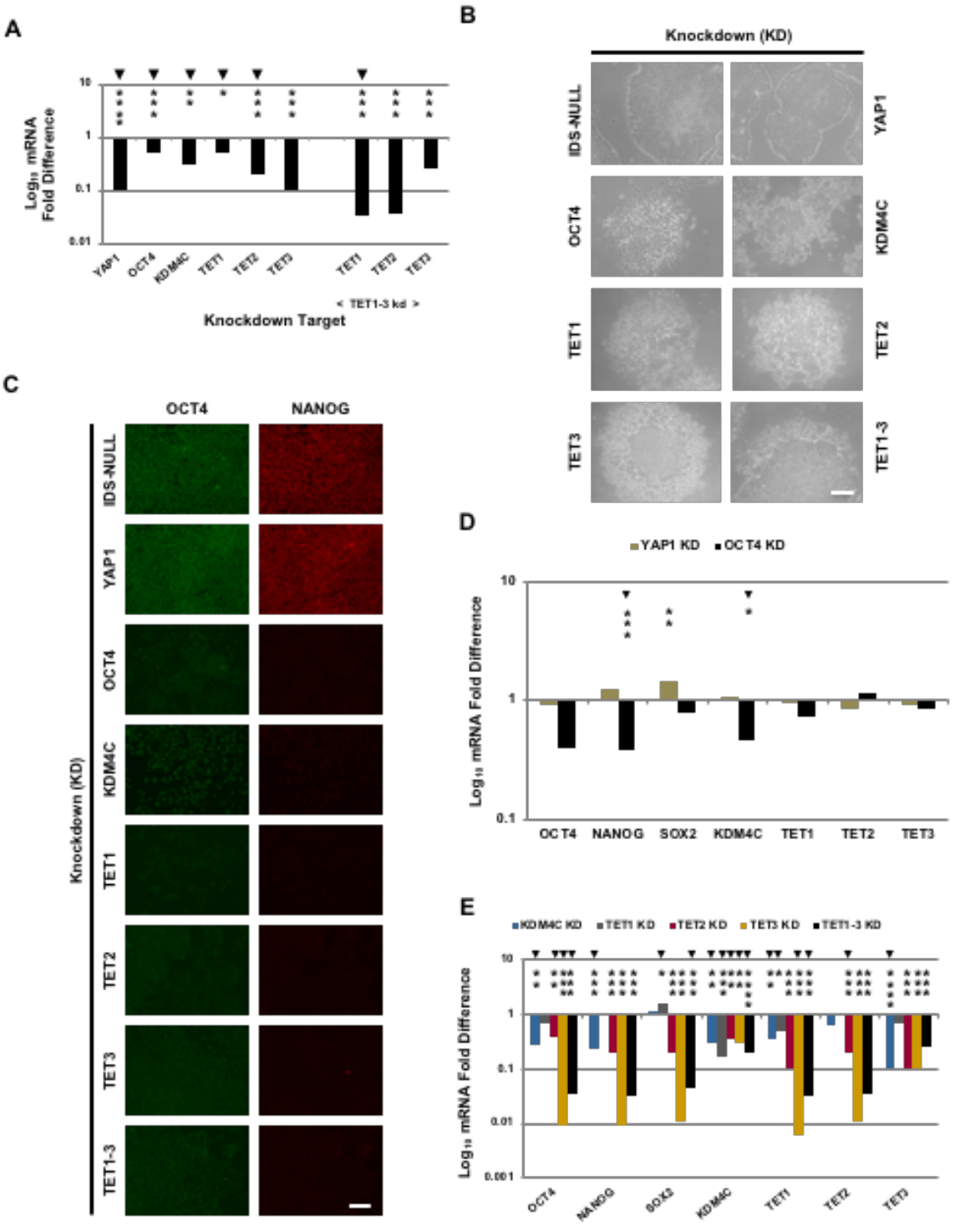

Figure 2. RNA interference targeting OCT4, KDM4C and TET1/2/3 perturbs morphological and molecular measures of pluripotency as assessed in H9 hESCs.

5

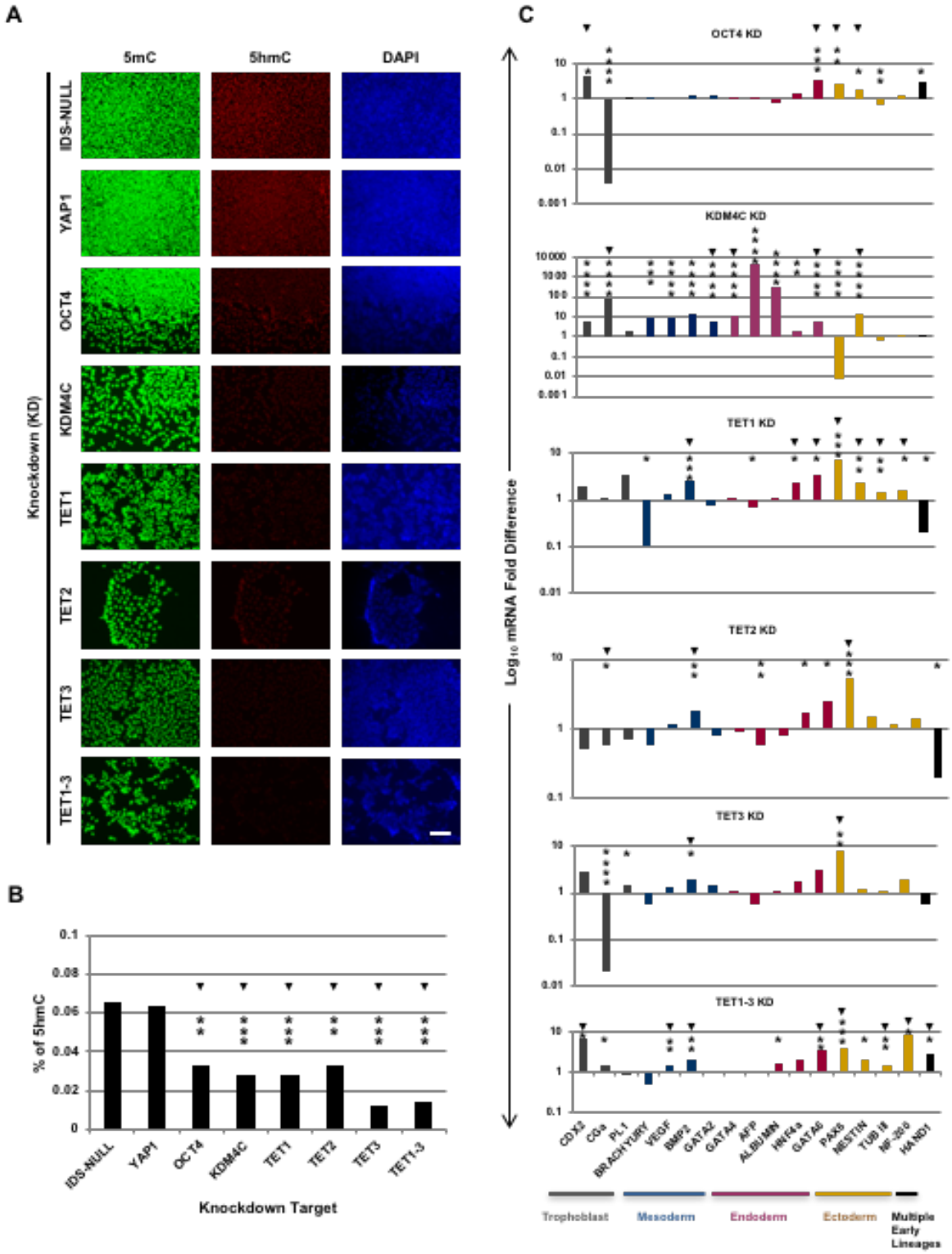

Figure 3. RNA interference targeting KDM4C and TET1/2/3 in H9 hESCs lowers genomic 5hmC content and induces differentiation associated alterations in lineage marker expression .

5

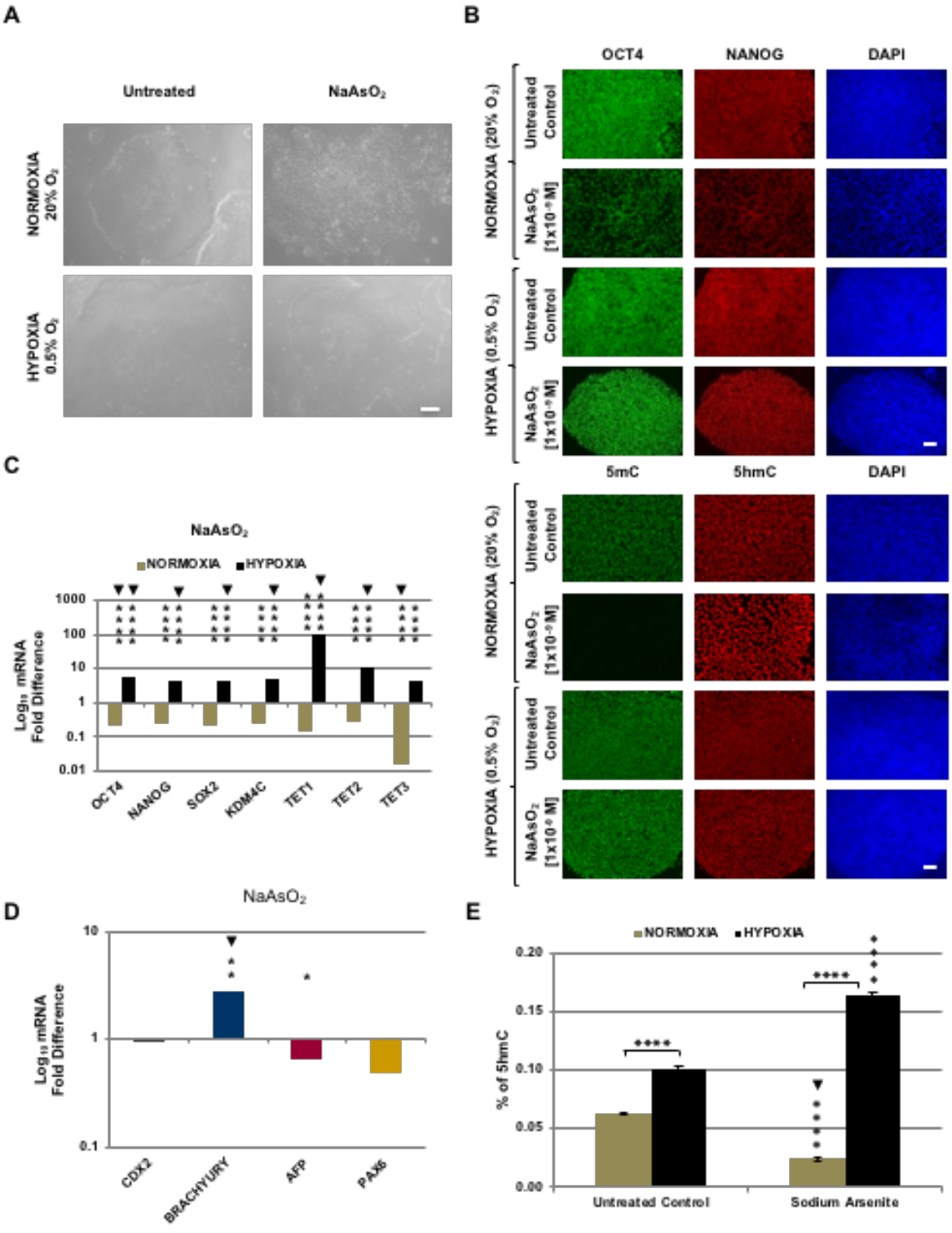

Figure 4. Differential effects of $NaAsO_2$ under normoxia vs hypoxia on measures of hESC phenotype and dioxygenase expression and function as assessed in H9 hESCs.

5

A

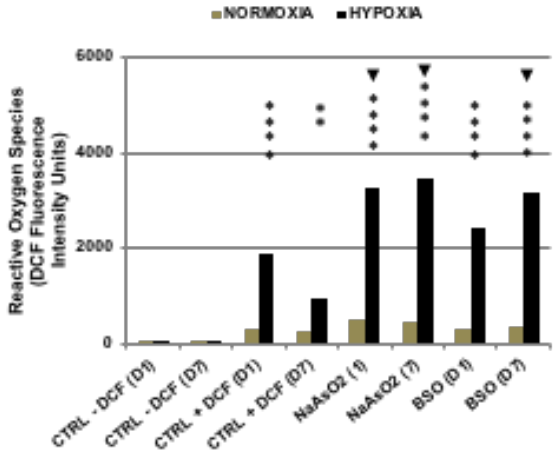

B

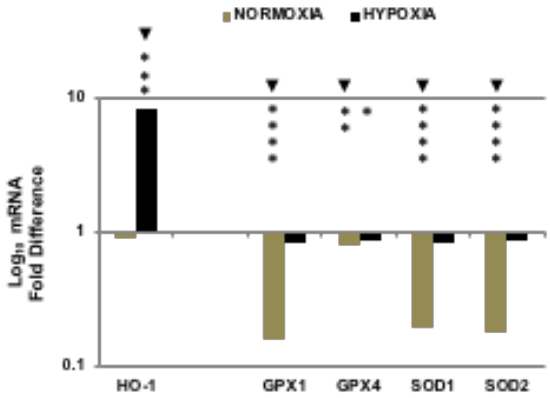

C

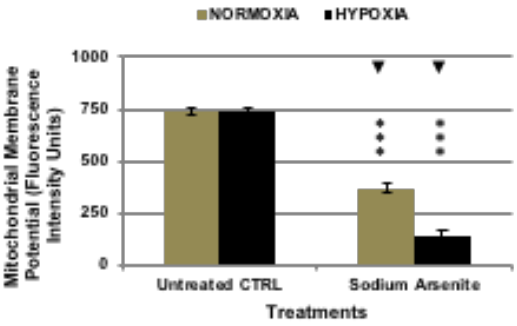

Figure 5. Differential effects of $NaAsO_2$ under normoxia vs hypoxia evident in measures of oxidative stress as assessed in H9 hESCs.

5

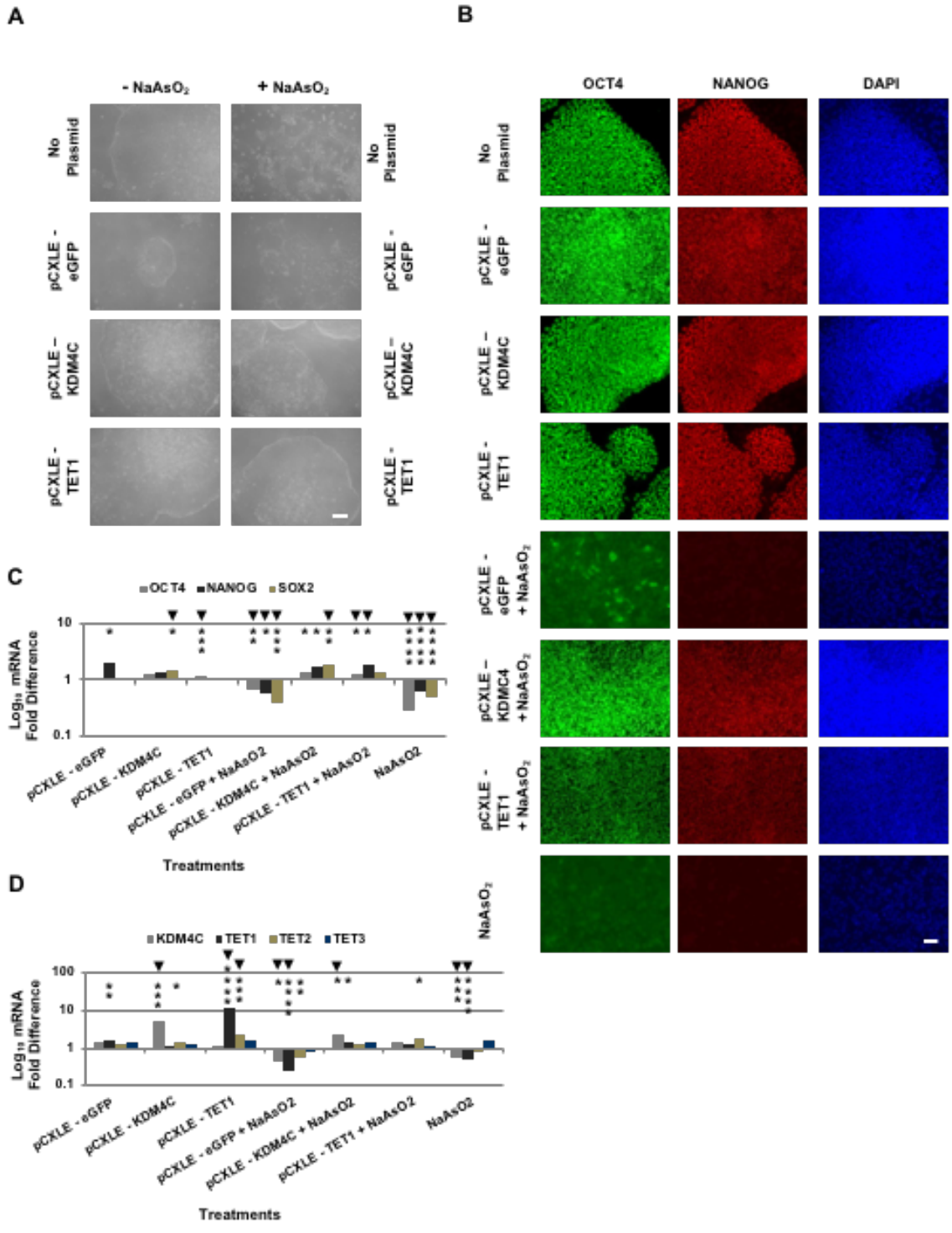

Figure 6. Transfection with plasmids encoding KDM4C or TET1 protects against $NaAsO_2$ induced differentiation under normoxia as assessed in H9 hESCs.

5

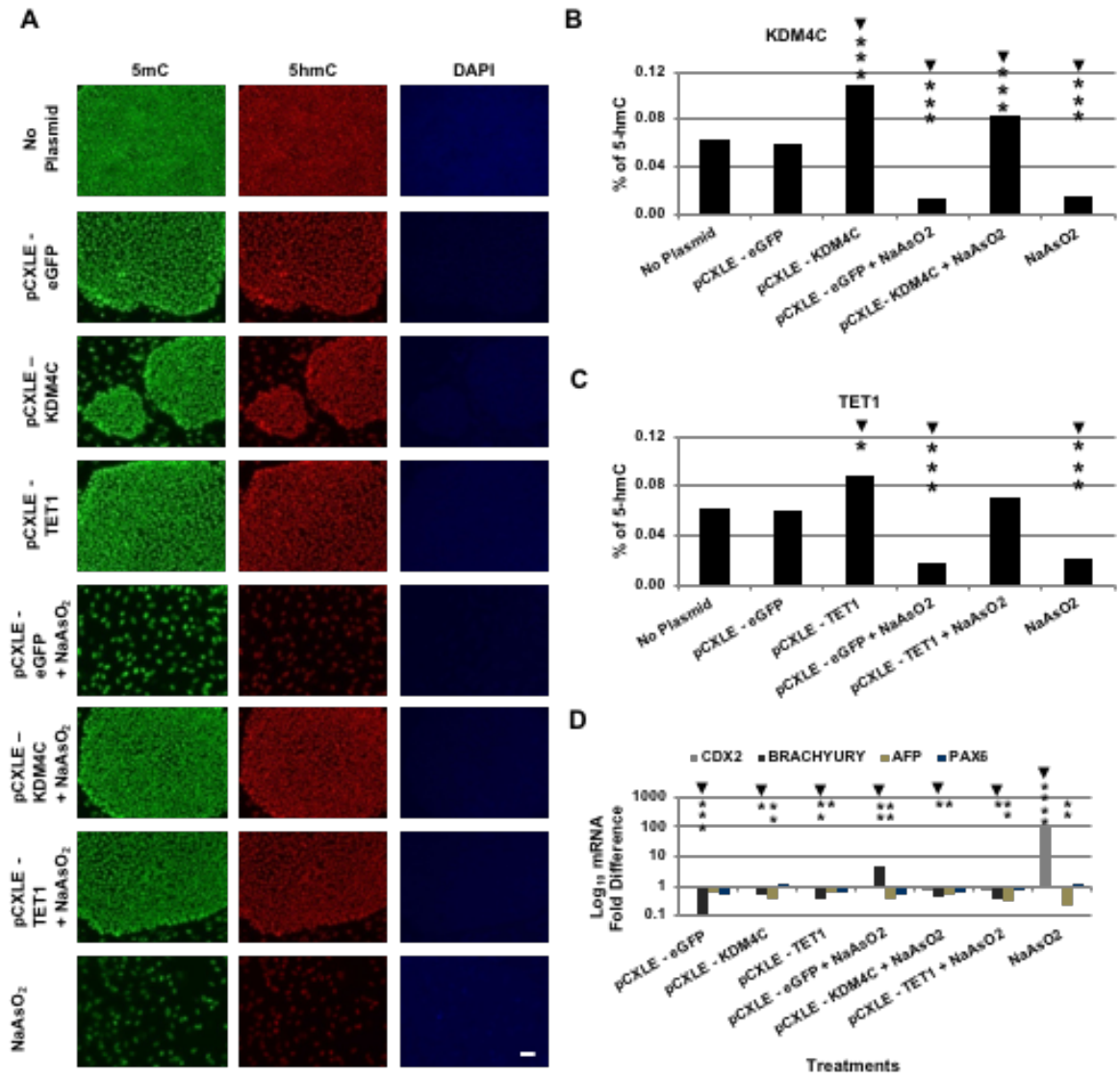

Figure 7. Transfection with plasmids encoding KDM4C or TET1 promotes genomic 5hmC content and inhibits differentiated lineage marker expression despite treatment with $NaAsO_2$ under normoxia as assessed in H9 hESCs.

5

Supplementary Information

Table of Contents

Supplementary Figure 1. Effect of hypoxia versus normoxia on measures of hESC phenotype, dioxygenase expression and function and oxidative stress as assessed in RH1 hESCs. (A) Compacted colony morphologies observed following 7 days of feeder-free cultivation under normoxia (21% O_2) vs hypoxia (0.5% O_2). Bar equals 100 µm. **(B)** Hypoxia enhances hESC growth over 7 days of cultivation. Bars depict the mean fold increase from day of seeding ± SD to each time point for each atmosphere (Seeding Density 20,000/cm^2; n=3). **(C)** Representative immunocytochemical detection of OCT4, NANOG, 5mC, 5hmC and fluorescent staining of nuclear DNA (DAPI) after 7 days of culture. Bar equals 100 µm. **(D)** ELISA quantification of 5hmC after 7 days of culture. Bar depicts mean ± SD (n=3). **(E)** Log_{10} fold change after 7 days in mRNA for pluripotency (OCT4, NANOG and SOX2) and dioxygenases (KDM4C, TET1, TET2 and TET3) in hypoxia relative to normoxia, set as 1 (n=4). **(F)** Generation of ROS at days 1 (D1) and 7 (D7) of culture under normoxia vs hypoxia assessed by flow cytometry detection of DCF dye fluorescence emission from stained (CTRL + dye) and unstained cells (CTRL - dye). Bars depict mean values ± SD of n= 6 (D1) and 7 (D7). **(G)** Hypoxia elevates steady state level of mRNA for HO-1 but not GPX1, GPX4, SOD1 and SOD2 assessed at 7 days of culture. Log_{10} fold increase in hypoxia treated cells relative to normoxia. set as 1 (n=4). **(H)** Mitochondrial membrane potential did not vary between cells cultured under both atmospheres for 7 days, as assessed by Rhodamine 123 fluorescence intensity. Bars represent mean fluorescence intensity ± SD (n=3). Conserved outcomes between cell lines (▼). Asterisks denote level of significance for representative outcomes for RH1 (*p<0.05; **p<0.01; ***p<0.001; ****p<0.0001).

Supplementary Figure 2. RNA interference targeting OCT4, KDM4C and TET1/2/3 perturbs morphological and molecular measures of pluripotency as assessed in RH1 hESCs. (A) Log_{10} fold change in steady state mRNA level of the siRNA targeted genes (YAP1, OCT4, KDM4C, TET1, TET2, TET3 and TET1-3 concurrently) expressed relative to cells transfected with random sequence derived from human IDS gene (IDS-NULL) (n=4). **(B)** Representative colony morphology corresponding to aforementioned siRNA transfections. Transfection with YAP1 and IDS-NULL siRNA have no effect on colony morphology, whereas targeting of OCT4, KDM4C, TET1-3 does. Bar equals 100 µm. **(C)** Immunocytochemistry for OCT4, NANOG corresponding to aforementioned transfections. Transfection with YAP1 and IDS-NULL siRNA have no qualitative effect on immunostaining for pluripotency markers whereas targeting of OCT4, KDM4C, TET1-3 does. Bar equals 100 µm. **(D)** Log_{10} fold change in steady state levels of mRNAs for pluripotency associated transcription factors (OCT4, NANOG, SOX2) and dioxygenases (KDM4C, TET1,2,3 and TET1-3) following siRNA targeting of YAP1 and OCT4 as above. Only targeting OCT4, results in significant changes in pluripotency or dioxygenase gene transcription. **(E)** Log_{10} fold change in steady state levels of mRNAs for pluripotency associated transcription factors (OCT4, NANOG, SOX2) and dioxygenases (KDM4C, TET1,2,3 and TET1-3) following siRNA targeting dioxygenases (n=4). Consistent with effects on morphology and OCT4 and NANOG immunocytochemistry, targeting all dioxygenases generally results in significant lowering of OCT4, NANOG and other dioxygenases. Conserved outcomes between cell lines (▼). Asterisks denote level of significance for representative outcomes for RH1 (*p<0.05; **p<0.01; ***p<0.001; ****p<0.0001).

Supplementary Figure 3. RNA interference targeting KDM4C and TET1/2/3 in RH1 hESCs lowers genomic 5hmC content and induces differentiation associated alterations in lineage marker expression. (A) Representative immunocytochemical detection of 5mC and 5hmC and fluorescent labelling of nuclear DNA (DAPI) following transfection with siRNAs directed against IDS-NULL, YAP1, OCT4, KDM4C, TET1, TET2, TET3 and TET1-3. Bar equals 100 µm. **(B)** ELISA quantification of 5hmC in siRNA treated cells. Bars represent mean percentage of genomic DNA +/- SD (n=3). **(C)** Log_{10} fold change in steady state mRNA levels after siRNA treatments expressed relative to cells transfected with random sequence derived from human IDS gene (IDS-NULL) set as 1 (n=4). Conserved outcomes between cell lines (▼). Asterisks denote level of significance for representative outcomes for RH1 (*p<0.05; **p<0.01; ***p<0.001; ****p<0.0001).

Supplementary Figure 4. Differential effects of $NaAsO_2$ under normoxia vs hypoxia on measures of hESC phenotype and dioxygenase expression and function as assessed in RH1 hESCs. (A) $NaAsO_2$ disrupts undifferentiated colony morphology under normoxia but not hypoxia. Bar equals 100 μm. **(B)** Representative immunofluorescent staining for OCT4, NANOG, 5mC, and 5hmC, and fluorescent staining for nuclear DNA (DAPI) following treatment with $NaAsO_2$ or not under normoxia or hypoxia. Bar equals 100 μm. **(C)** Log_{10} fold change in levels of mRNA for OCT4, NANOG, SOX2, KDM4C, TET1, TET2 and TET3 following treatment with $NaAsO_2$ under normoxia or hypoxia expressed relative to untreated cells in the same atmosphere, set as 1 (n=4). **(D)** Log_{10} fold change in levels of mRNA for germinal lineage markers CDX2, BRACHYURY, AFP and PAX6 under normoxia following treatment with $NaAsO_2$ expressed relative to untreated cells set as 1 (n=4). **(E)** ELISA quantification of 5hmC in $NaAsO_2$ treated and untreated cells in normoxia vs hypoxia. Bars represent mean +/- SD (n=3). Conserved outcomes between cell lines (▼). Asterisks denote level of significance for representative outcomes for RH1 (*p<0.05; **p<0.01; ***p<0.001; ****p<0.0001).

Supplementary Figure 5. Differential effects of $NaAsO_2$ under normoxia vs hypoxia evident in measures of oxidative stress as assessed in RH1 hESCs. (A) Generation of ROS at days 1 (D1) and 7 (D7) of culture following treatment or not with $NaAsO_2$ under normoxia vs hypoxia. ROS were determined by flow cytometry detection of DCF dye fluorescence emission from stained (CTRL + dye) and unstained cells (CTRL - dye) cells. Bars depict mean values ± SD of n= 6 (D1) and 7 (D7). **(B)** Log_{10} fold change in levels of mRNA for HO-1, and antioxidants GPX1, GPX4, SOD1, SOD2 in $NaAsO_2$ treated cells under normoxia vs hypoxia expressed relative to values in untreated cells, set as 1 (n=4). **(C)** Mitochondrial membrane potential in $NaAsO_2$ treated and untreated control cells under normoxia or hypoxia. Bars represent mean Rhodamine 123 fluorescence intensity ± SD (n=4). Conserved outcomes between cell lines (▼). Asterisks denote level of significance for representative outcomes for RH1 (*p<0.05; **p<0.01; ***p<0.001; ****p<0.0001).

Supplementary Figure 6. Transfection with plasmids encoding KDM4C or TET1 protects against $NaAsO_2$ induced differentiation under normoxia as assessed in RH1 hESCs. (A) Compacted colony morphology is protected by transfection with plasmids (pCXLE-) encoding KDM4C and TET1 but not eGFP, or exposed to transfection reagents only prior to treatment with $NaAsO_2$ under normoxia. Bar equals 100 μm. **(B)** Immunofluorescent staining for OCT4 and NANOG correlate with aforementioned effects on colony morphology. Bar equals 100 μm. Corresponding cell nuclei depicted by DAPI staining. **(C)** Log_{10} fold change in mRNA for OCT4, NANOG, SOX2 in aforementioned treatment groups depicted relative to untreated control (no plasmid) set as 1 (n=4). **(D)** Log_{10} fold change in mRNA for KDM4C, TET1, TET2 and TET3 in aforementioned treatment groups depicted relative to untreated control (no plasmid) set as 1 (n=4). Conserved outcomes between cell lines (▼). Asterisks denote level of significance for representative outcomes for RH1 (*p<0.05; **p<0.01; ***p<0.001; ****p<0.0001).

Supplementary Figure 7. Transfection with plasmids encoding KDM4C or TET1 promotes genomic 5hmC content and inhibits differentiated lineage marker expression despite treatment with $NaAsO_2$ under normoxia as assessed in RH1 hESCs. (A) Immunofluorescent staining for 5mC and 5hmC correlate with aforementioned effects on colony morphology. Bar equals 100 μm. Corresponding cell nuclei depicted by DAPI staining. **(B)** ELISA quantification of 5-hmC in pCXLE-KDM4C transfection experiment. Bars represent mean +/- SD (n=3). **(C)** ELISA quantification of 5hmC in pCXLE -TET1 transfection experiment. Bars represent mean +/- SD (n=3). **(D)** Log_{10} fold change in mRNA for CDX2, BRACHYURY, AFP, and PAX6 following transfection of pCXLE -eGFP, KDM4C, and TET1, or no plasmid (transfection reagents) and treatment with $NaAsO_2$ depicted relative to untreated (and no plasmid) control set as 1 (n=4). Conserved outcomes between cell lines (▼). Asterisks denote level of significance for representative outcomes for RH1 (*p<0.05; **p<0.01; ***p<0.001; ****p<0.0001).

Supplementary Figure 8. Confirmation that treatment with N-acetyl-L-cysteine (+ NAC) promotes maintenance of undifferentiated hESC colony morphology and genomic 5hmC content despite treatment with sodium arsenite ($NaAsO_2$) under normoxia and hypoxia as assessed in (A) H9 and (B) RH1 hESCs. Supplementation of hESC culture media with N-acetyl-L-cysteine, a potent antioxidant, maintains the undifferentiated hESC colony morphology and genomic 5hmC content upon exposure to $NaAsO_2$ under normoxia and hypoxia. Immunofluorescent staining for OCT4, NANOG, 5mC, and 5hmC, and fluorescent staining for nuclear DNA (DAPI) following antioxidant treatment with and without $NaAsO_2$ under normoxia and hypoxia. Bar equals 100 μm.

Supplementary Figure 9. Confirmation effect of sodium arsenite ($NaAsO_2$) treatment on measures of pluriptency and 2OG dioxygenase gene (A) and lineage marker (B) expression. and genomic 5hmC content (C) under normoxia vs hypoxia following concurrent antioxidant treatment with N-acetyl-L-cysteine (NAC), as assessed in (i) H9 and (ii) RH1 hESCs. (A) Log_{10} fold change in mRNA for pluripotency (OCT4, NANOG and SOX2) and dioxygenases (KDM4C, TET1, TET2 and TET3) under normoxia and hypoxia following antioxidant treatment with NAC as assessed by RTq-PCR depicted relative to non-$NaAsO_2$ treatments in the presence or absence of NAC set as 1 (n=4). **(B)** Log_{10} fold change in levels of mRNA for germinal lineage markers CDX2, BRACHYURY, AFP and PAX6 under normoxia following antioxidant treatment with NAC depicted relative to non-$NaAsO_2$ treatments, set as 1 (n=4). **(C)** ELISA quantification of 5hmC in untreated and $NaAsO_2$-treated hESCs following antioxidant treatment with NAC under normoxia and hypoxia. Bars represent mean +/- SD (n=3). For (A and B) significance of differences in fold change between NAC-treated cells vs non-NAC-treated cells in each atmosphere is shown. For C, significance of differences within atmospheres and presence/absence of NAC is shown. Conserved outcomes between cell lines (▼). Asterisks denote level of significance for representative outcomes for H9 and RH1 (*p<0.05; **p<0.01; ***p<0.001; ****p<0.0001).

Supplementary Figure 10. Confirmation of differential effects of sodium arsenite ($NaAsO_2$) on hESC under normoxia vs hypoxia evident with or without N-acetyl-L-cysteine (NAC) on reactive oxygen species production (A), antioxidant gene expression (B), and mitochondrial membrane potential (C) as assessed in (i) H9 and (ii) RH1 hESCs. **(A)** Generation of ROS at days 1 (D1) and 7 (D7) of culture under normoxia vs hypoxia following antioxidant treatment with N-acetyl-L-cysteine as assessed by flow cytometry detection of DCF dye fluorescence emission from stained (CTRL + dye) and unstained cells (CTRL - dye). Buthionine Sulfoximine (BSO) is known to elevate ROS. **(B)** Log_{10} fold change in levels of mRNA Levels for HO-1, GPX1, GPX4, SOD1 and SOD2 assessed at 7 days of culture depicted relative to non-NAC-treated, set as 1 (n=4). **(C)** Mitochondrial membrane potential in untreated and $NaAsO_2$-treated cells cultured under both atmospheres for 7 days, as assessed by Rhodamine 123 fluorescence intensity. Bars represent mean fluorescence intensity ± SD (n=3).). For (A) significance of differences between atmospheres is shown. For (B) significance of differences in fold change between NAC- vs non-NAC-treated cells in each atmosphere is shown. For C, significance of differences in mitochondrial membrane potential between $NaAsO_2$–treated -vs non-treated controls, within each is shown. Asterisks denote level of significance (*p<0.05; **p<0.01; ***p<0.001; ****p<0.0001), with conserved outcomes between cell lines denoted by inverted triangle (▼).

Supplementary Figure 11. Statistical analysis of the effects of antioxidant treatment under normoxia and hypoxia on levels of (A) reactive oxygen species (ROS) and (B) mitochondrial membrane potential (MMP) in (i) H9, (ii) RH1 and (iii) H9 and RH1 hESCs. For each cell line and each day of assessment (D1 or 7), a one-way ANOVA was performed comparing effect of atmosphere (normoxia vs hypoxia) vs treatment (untreated alone, untreated+NAC, $NaAsO_2$ alone, $NaAsO_2$+NAC, BSO alone, BSO+NAC,), followed by Tukey post test for which *p* values are presented for the normoxia vs normoxia+NAC and hypoxia vs hypoxia+NAC comparisons. A t-test was performed for the normoxia vs hypoxia comparison.

Supplementary Figure 12. Establishment of $NaAsO_2$ concentration treatment cytotoxicity range following continuous exposure of hESCs over seven days. Eleven concentrations of $NaAsO_2$ over a 3 log-fold range (H9: $1x10^{-9}$ – $1x10^{-12}$ M; RH1: $3.3x10^{-11}$ – $3.3x10^{-14}$ M), based on previously reported toxicity ranges for other cells was evaluated for effect on the viability of H9 (A) and RH1 (B). For each concentration to be tested cells were first seeded in the absence of $NaAsO_2$ in triplicate replicate feeder-free cultures in a 96-well plate format at 1 x 10^4 per well (surface area per well: 0.32 cm^2). After 24 hours media was replaced with that containing a specified concentration of $NaAsO_2$ and cultivated over 7 days in 5% CO_2 in air (21% O_2) at 37^oC, with medium replaced every 2 days. At the endpoint of culture viable cell numbers were assessed using a CellTiter-Blue® Cell Viability Assay (Promega, Cat No. G8080). Shown are mean +/- SD viable cell numbers in relation to treatment concentration. Curves depict regressions of mean values fitted by four parametric hill function using GraphPad Prism software (San Diego, CA, USA). From these the inhibitory concentration causing a ten percent reduction in viability (IC_{10}) normalised to untreated cell cultures were determined for use in subsequent experiments. Cytotoxicity range finder experiments were independently confirmed in each cell line (data not shown).

Supplementary Figure 13. Primary and secondary antibodies used in the study, target, source and dilution.

Supplementary Figure 14. Oligonucleotide primer sequences for genes assessed by RT-qPCR. These were designed in house (De Sousa laboratory) or acquired from the laboratory of Prof. A. Sachinidis or adapted from other published studies (Danet et al., 2003; Piccoli et al., 2007).

Supplementary Figure 15. Schematic illustration of the siRNA-mediated knockdown experiments. H9 and RH1 hESCs were transfected twice at a 24-hour interval with siRNA directed against the mRNA of YAP1, OCT4, KDM4C, TET1, TET2, TET3 and all three TETs (TET1-3). All cultures were maintained under feeder-free conditions in mTeSR-1. Samples were collected for RT-qPCR, immunocytochemistry and ELISA. Abbreviation/Acronym: 12-w, 12-well; siRNA, small interfering RNA.

Supplementary Figure 16. Episomal plasmids derived for the ectopic expression of epigenetically-marked 2-oxoglutarate-dependent dioxygenases. Maps of the episomal expression plasmids created for the ectopic expression of TET1 and KDM4C in H9 and RH1 hESCs.

Supplementary Figure 17. ***StemCellNet* network analysis of regulatory and physical interactions with TET1-3 and KDM4C 2-oxoglutarate dioxygenases.** We interrogated an interactive platform for retrieval and analysis of molecular networks associated with stem cells and their marker genes, *StemCellNet* (http://stemcellnet.sysbiolab.eu; [49]) to assess associations between dioxygenases in our study and pluripotency and non-pluripotency gene products, without **(A)**, or with **(B)** mapping to stemness gene sets. Molecules are depicted as yellow circles in A, or circles and square in B, latter denoting non-stemness genes according to studies on which the *StemCellNet* database is based. Mapping stemness gene sets in B re-sizes the nodes so that the their size is proportional to the number of sets they belong to. The dioxygenases (defined as hubs with grey circles, or squares) appear to have a total of at least 52 physical (blue line) and 26 regulatory (red arrow) molecular interactions, of which 23 and 10, respectively are stemness gene associated. All

dioxygenases physically interact or are transcriptionally regulated by a minimum of 3 (ie. TET3) and as many as 26 (ie. KDM4) stemness associated genes. OCT4, NANOG and SOX2 all directly regulate KDM4C and TET2. OCT4 and NANOG also physically interact with TET1. The transcription factors SMAD2 and 3, downstream of TGF-β/activin type 1 receptor signal transduction, regulate TET1, TET3 and KDM4C.

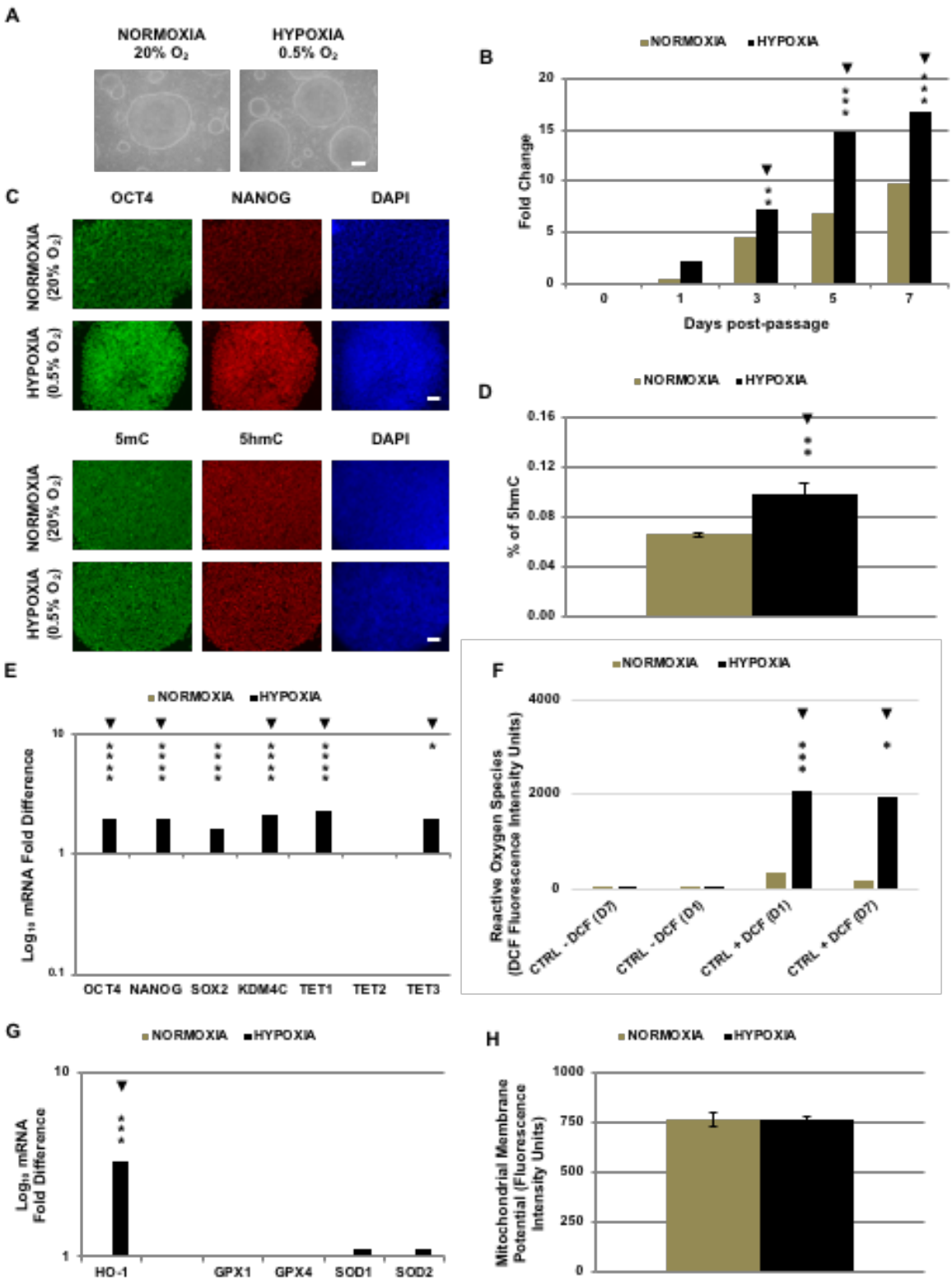

Supplementary Figure 1. Confirmation of effect of hypoxia versus normoxia on measures of hESC phenotype, dioxygenase expression and function and oxidative stress assessed in RH1 hESC.

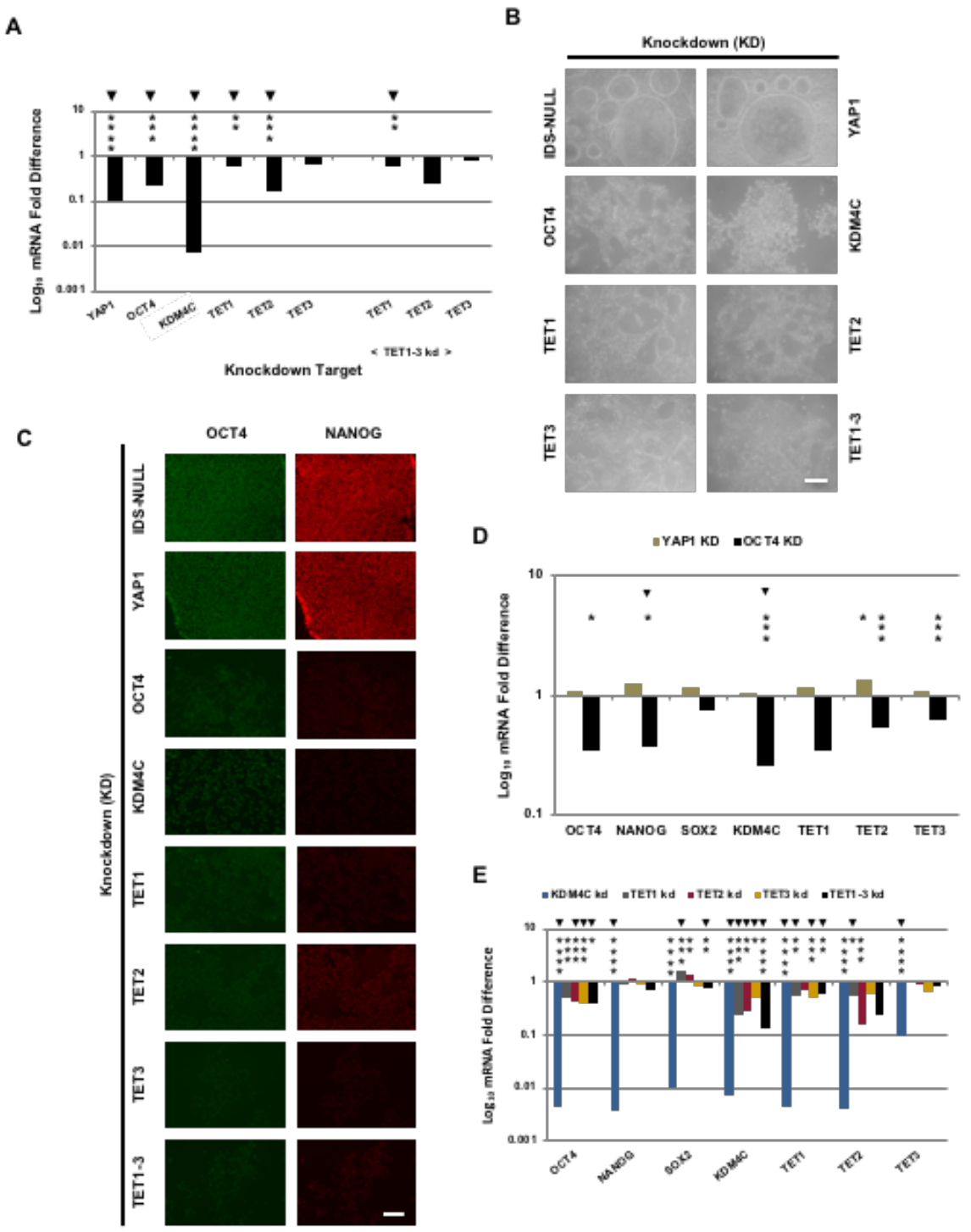

Supplementary Figure 2. RNA interference targeting OCT4, KDM4C and TET1/2/3 perturbs undifferentiated colony morphology and expression of pluripotency associated transcription factors and dioxygenases as assessed in RH1 hESC.

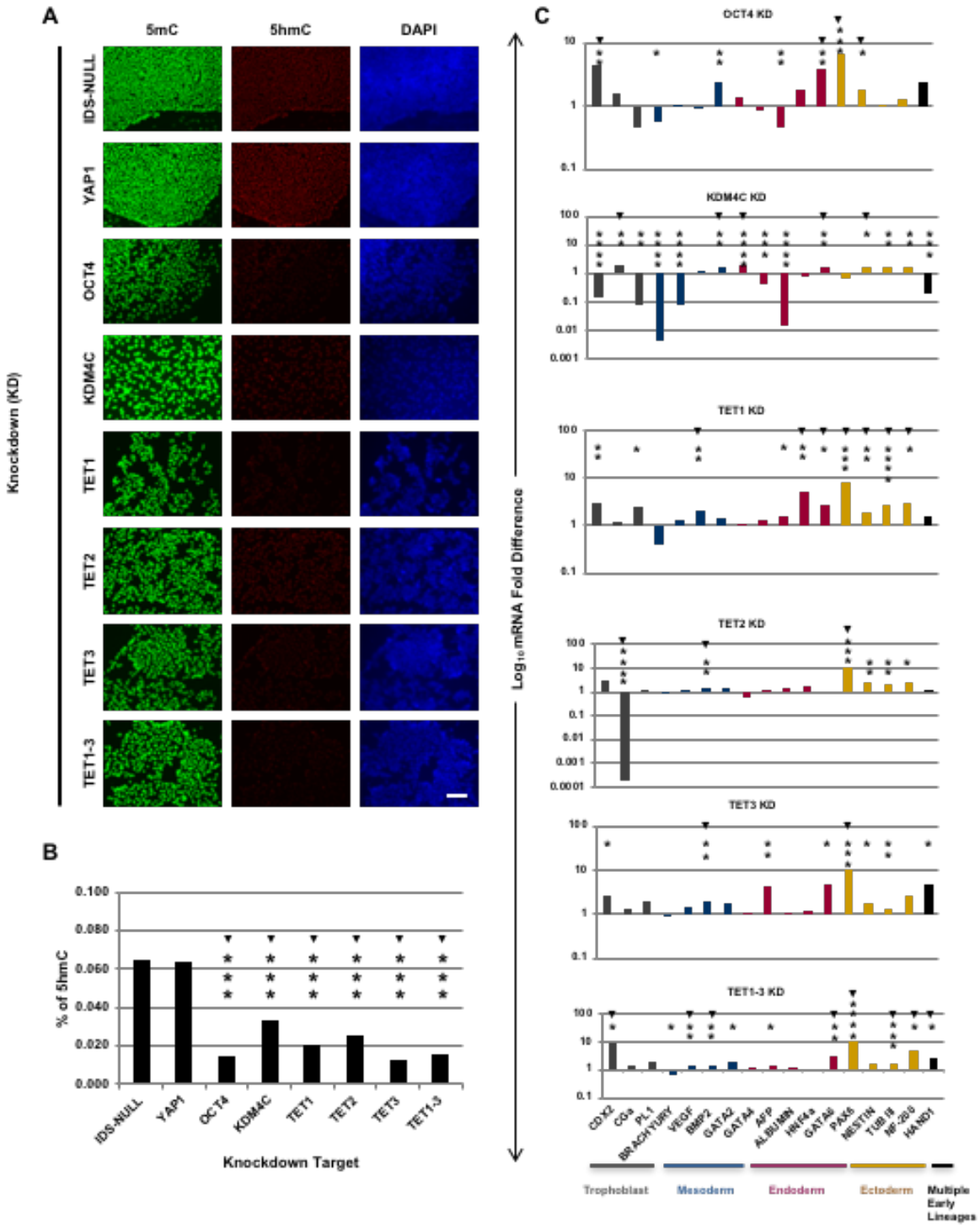

Supplementary Figure 3. Confirmation that RNA interference targeting KDM4C and TET1/2/3 lowers genomic 5hmC content and induces differentiation associated alterations in lineage marker expression as assessed in RH1 hESC.

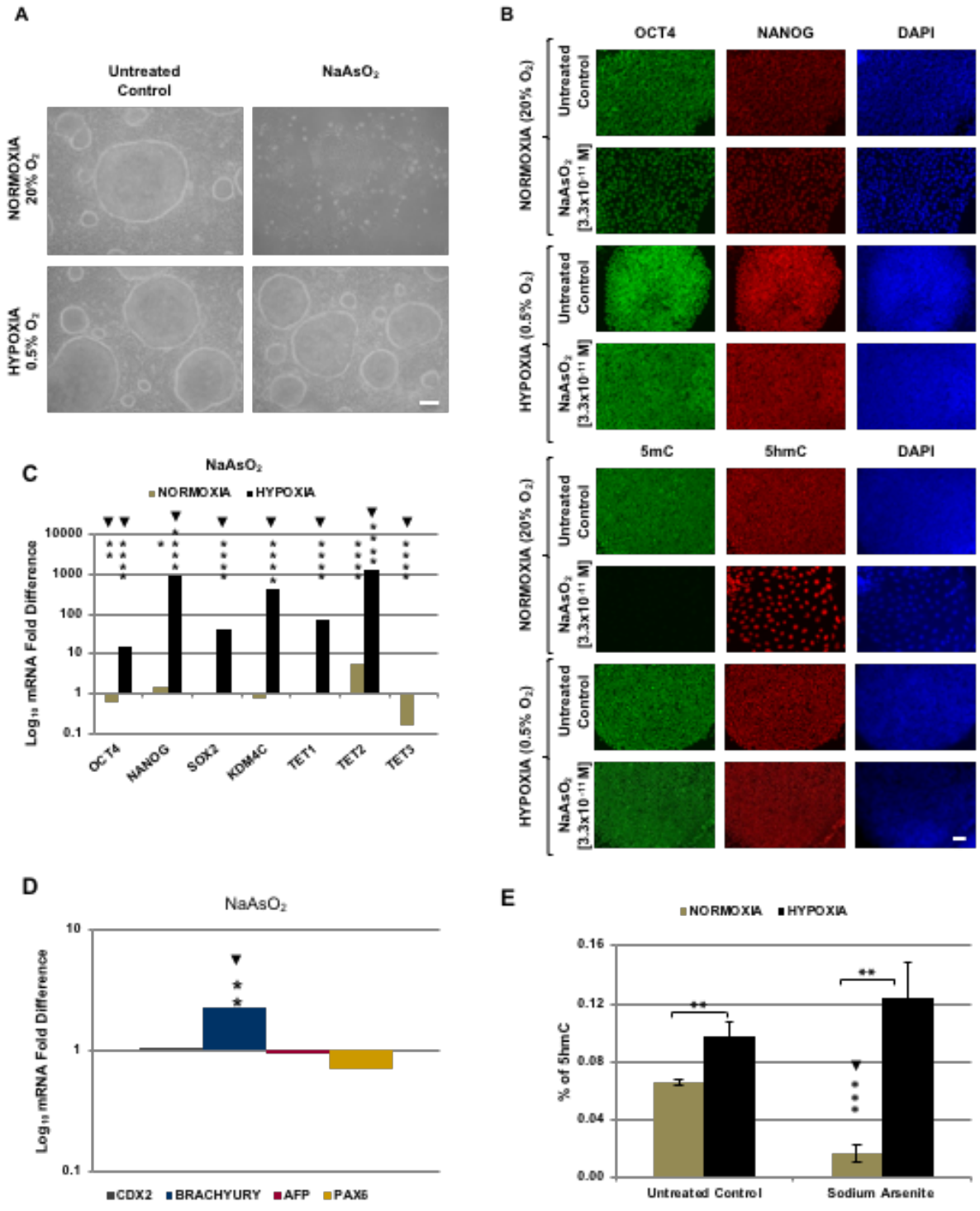

Supplementary Figure 4. Confirmation of differential effects of $NaAsO_2$ under normoxia vs hypoxia on undifferentiated colony morphology, genomic 5hmC content and expression of pluripotency associated transcription factors, dioxygenases and lineage markers as assessed in RH1 hESC.

A

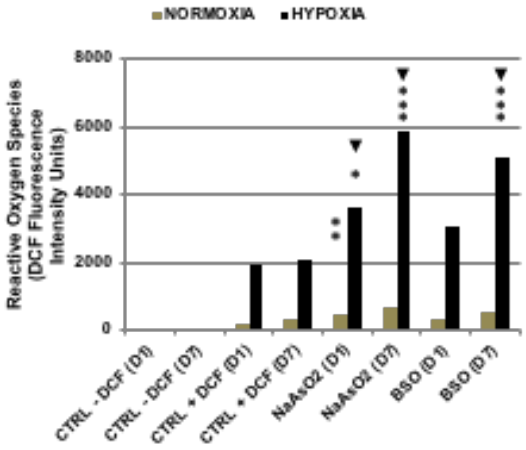

B

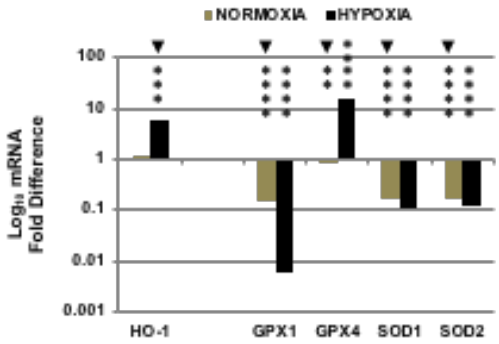

C

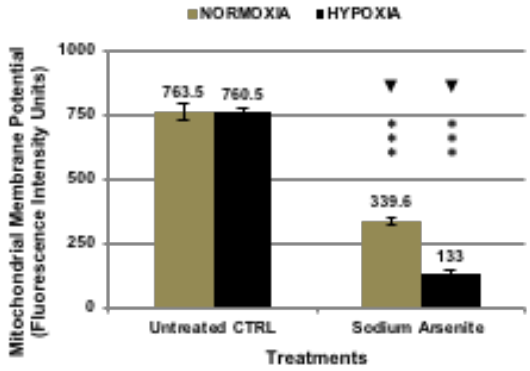

Supplementary Figure 5. Confirmation of differential effects of sodium arsenite ($NaAsO_2$) on hESC under normoxia vs hypoxia evident in measures of oxidative stress as assessed in RH1 hESC.

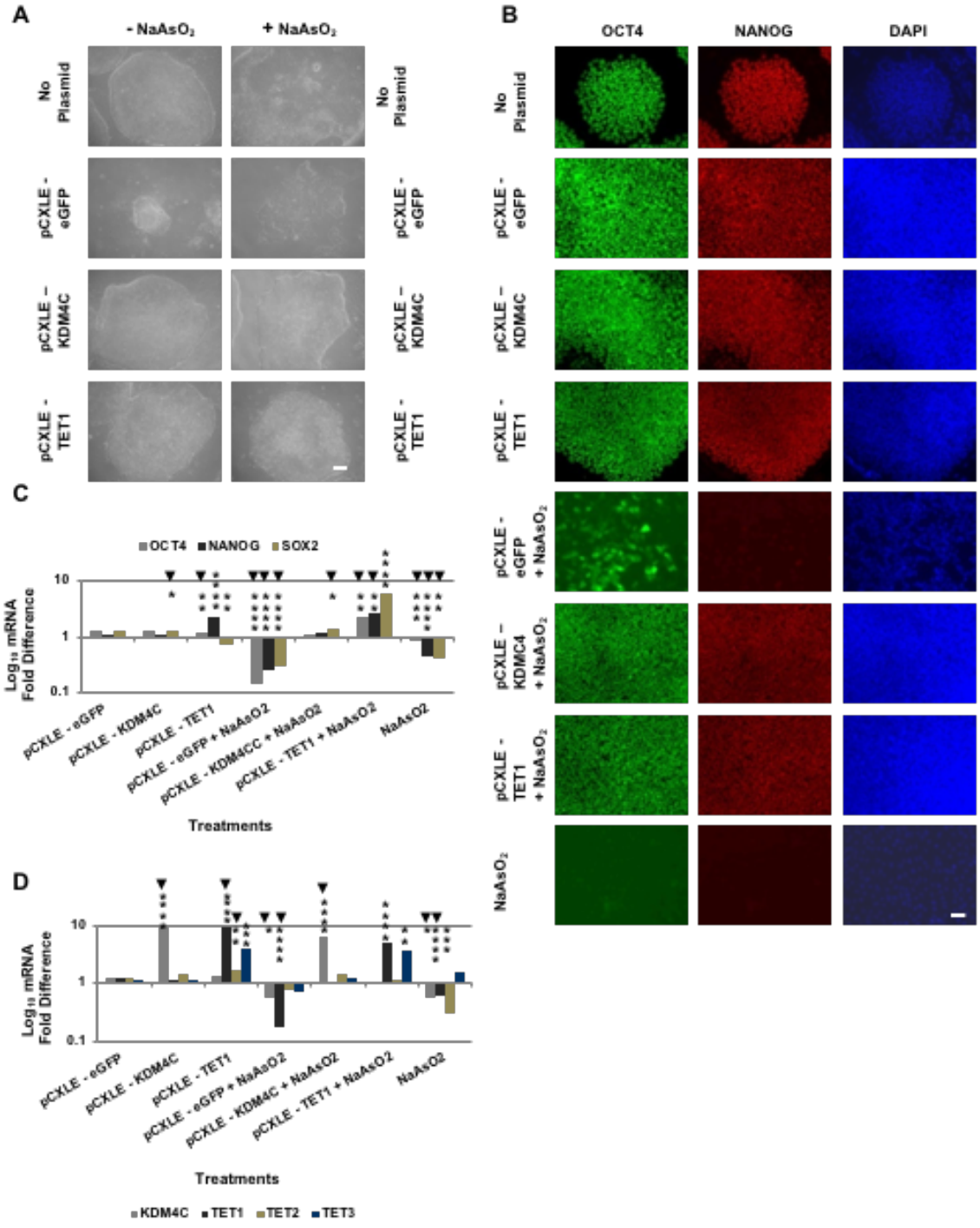

Supplementary Figure 6. Confirmation that transfection with plasmids encoding KDM4C or TET1 promotes maintenance of undifferentiated hESC colony morphology, and expression of pluripotency genes despite treatment with sodium arsenite ($NaAsO_2$) under normoxia as assessed in RH1 hESC.

5

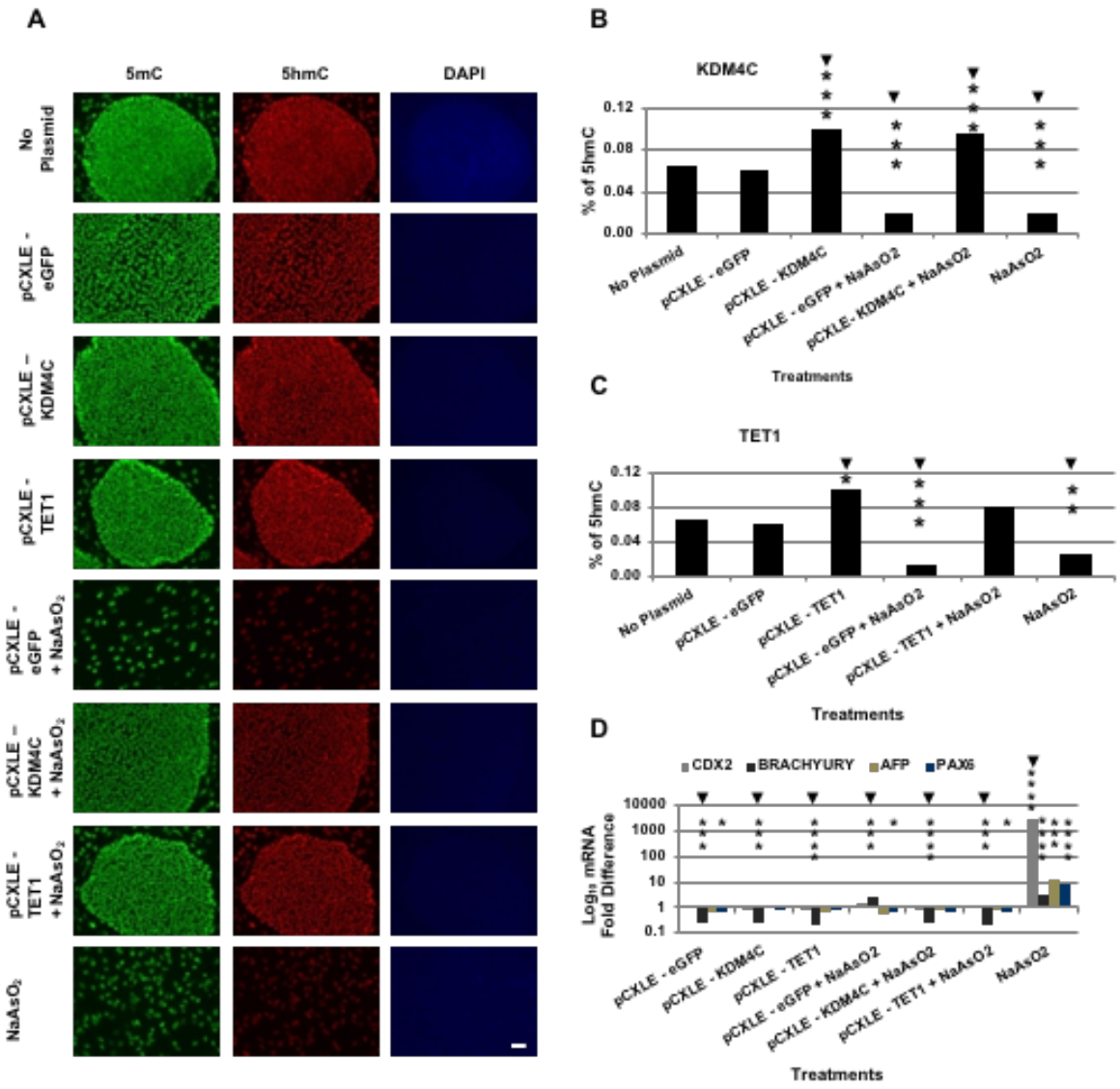

Supplementary Figure 7. Confirmation that transfection with plasmids encoding KDM4C or TET1 promotes genomic 5hmC content and inhibits differentiated lineage marker expression despite treatment with sodium arsenite ($NaAsO_2$) under normoxia as assessed in RH1 hESC.

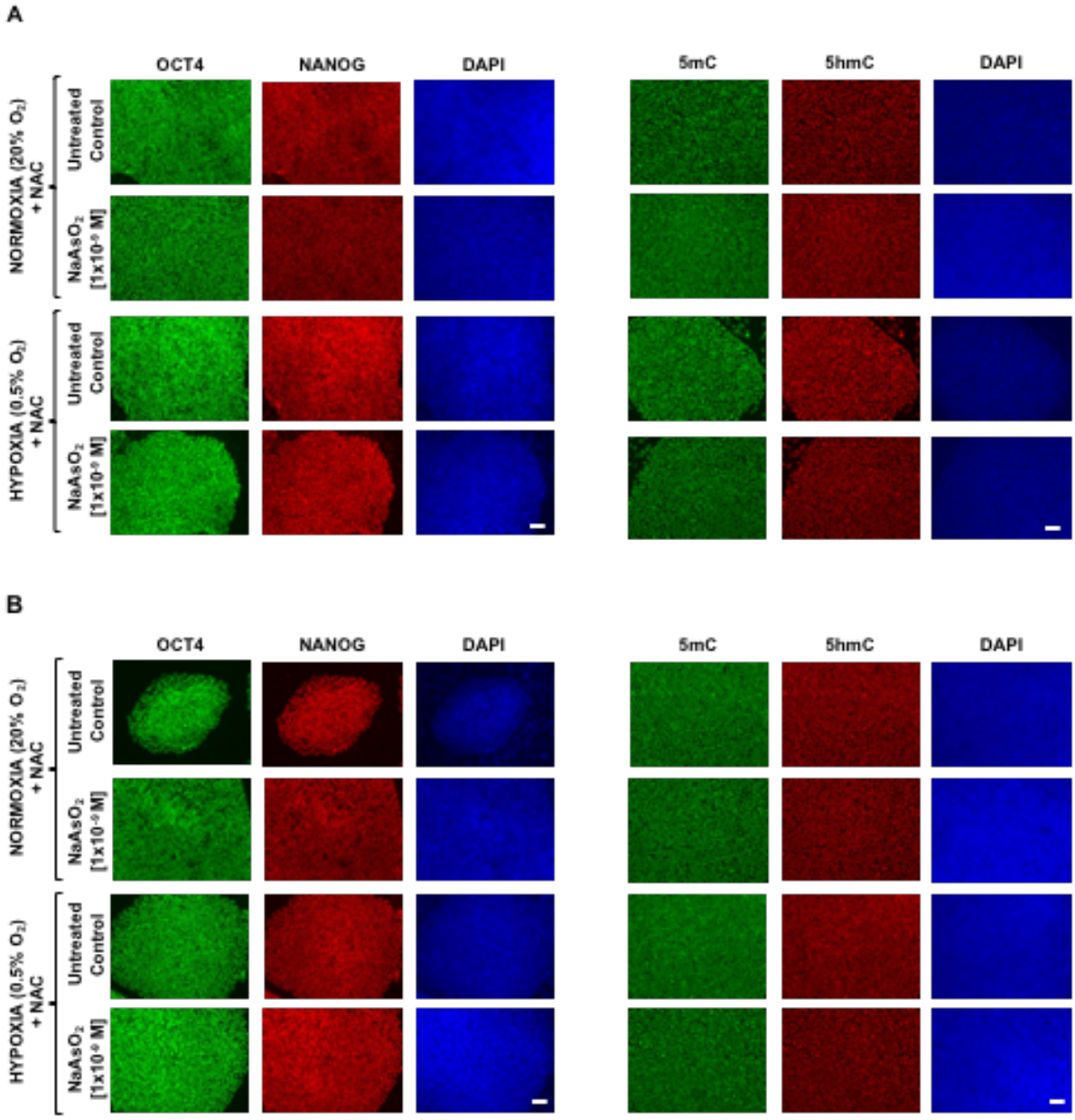

Supplementary Figure 8. Confirmation that treatment with N-acetyl-L-cysteine (+ NAC) promotes maintenance of undifferentiated hESC colony morphology and genomic 5hmC content despite treatment with sodium arsenite ($NaAsO_2$) under normoxia and hypoxia as assessed in (A) H9 and (B) RH1 hESCs.

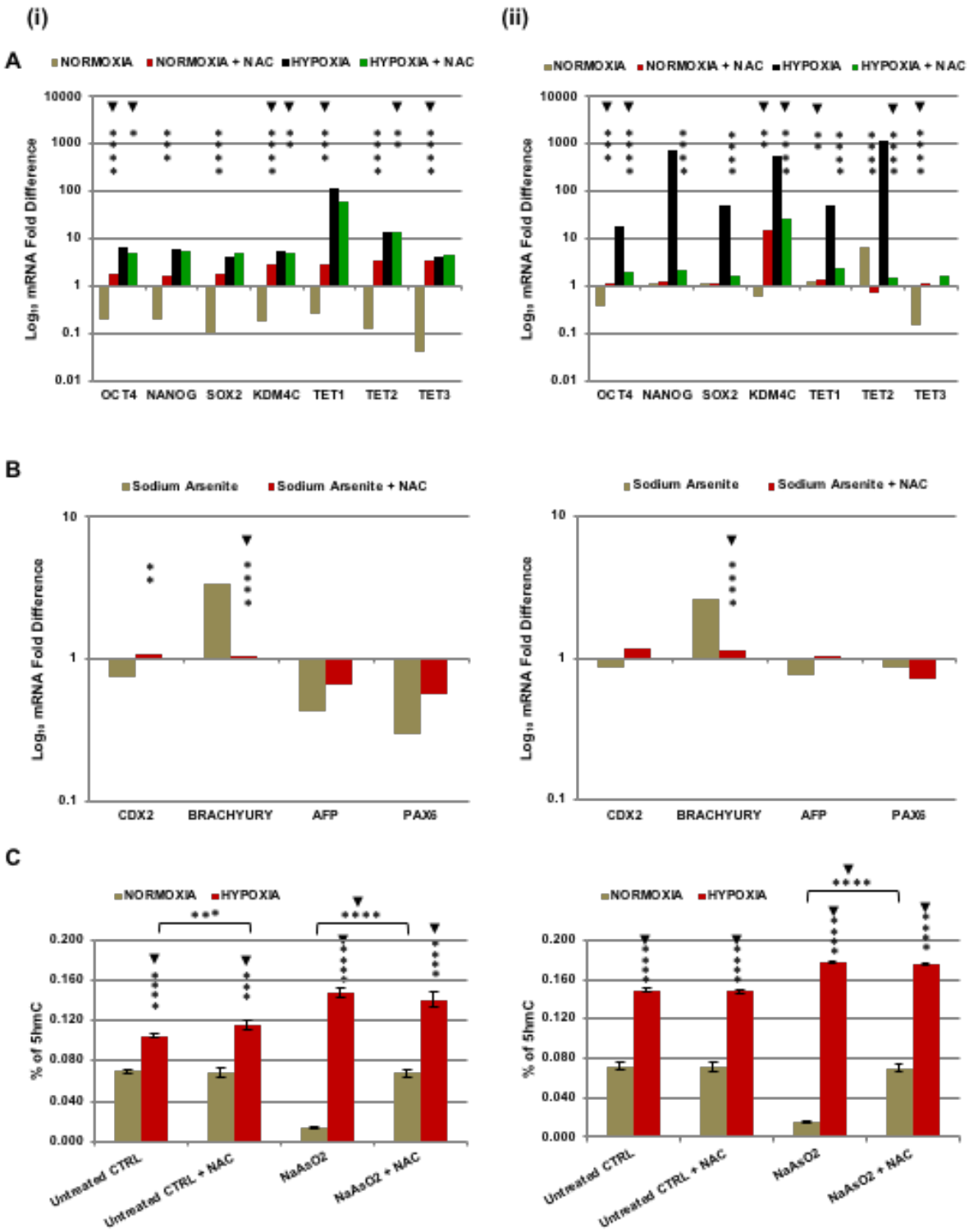

Supplementary Figure 9. Confirmation effect of sodium arsenite ($NaAsO_2$) treatment on measures of pluriptency and 2OG dioxygenase gene (A) and lineage marker (B) expression. and genomic 5hmC content (C) under normoxia vs hypoxia following concurrent antioxidant treatment with N-acetyl-L-cysteine (NAC), as assessed in (i) H9 and (ii) RH1 hESCs.

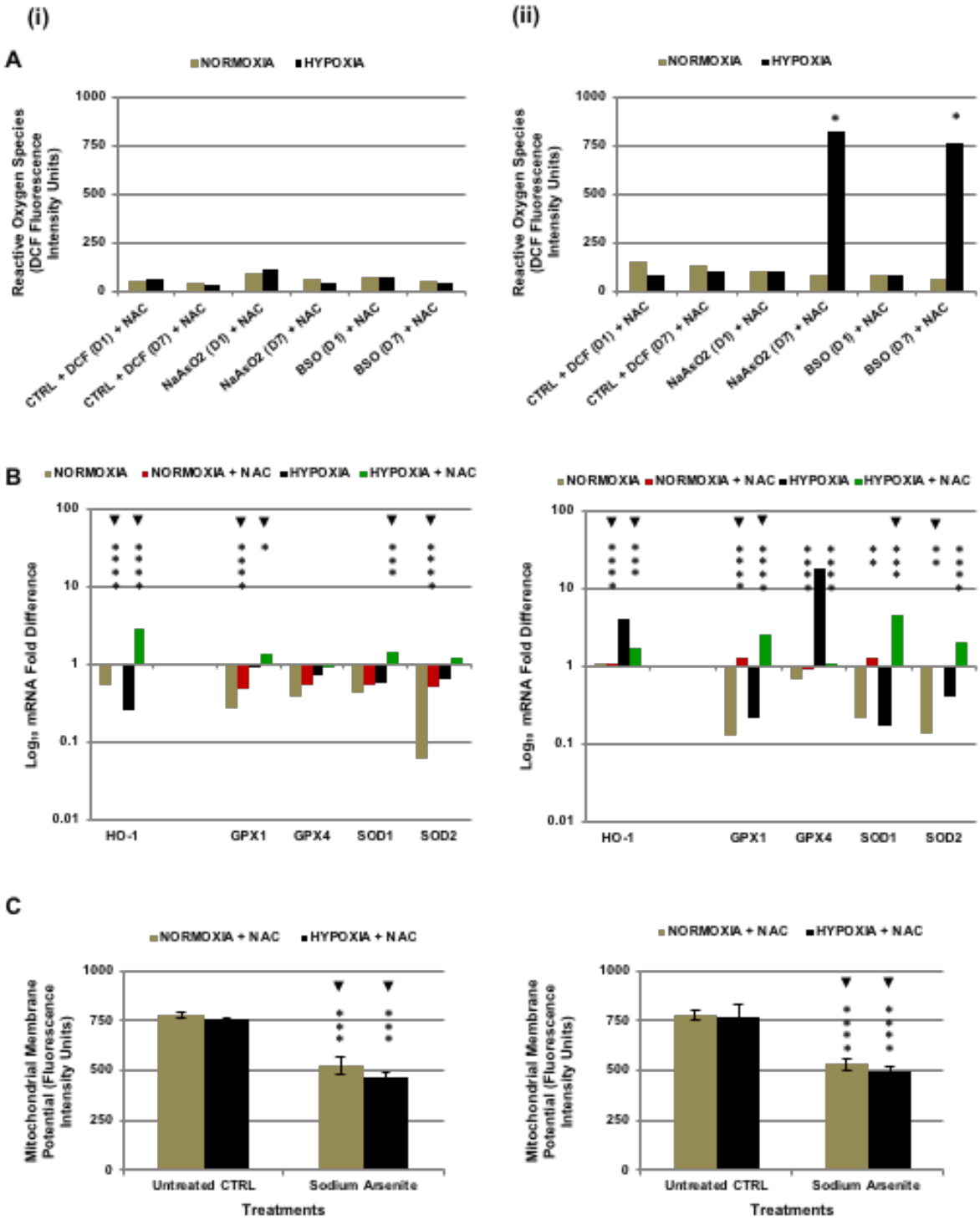

Supplementary Figure 10. Confirmation of differential effects of sodium arsenite ($NaAsO_2$) on hESC under normoxia vs hypoxia evident with or without N-acetyl-L-cysteine (NAC) on reactive oxygen species production (A), antioxidant gene expression (B), and mitochondrial membrane potential (C) as assessed in (i) H9 and (ii) RH1 hESCs.

A (i)

TREATMENT GROUP	DAY OF CULTURE	NORMOXIA + NAC vs NORMOXIA	HYPOXIA + NAC vs HYPOXIA	NORMOXIA vs HYPOXIA
CTRL + DCF	1	Not Significant	P < 0.001	P < 0.0001
	7	Not Significant	P < 0.05	P < 0.01
$NaAsO_2$	1	P < 0.01	P < 0.001	P < 0.0001
	7	P < 0.01	P < 0.001	P < 0.0001
BSO	1	Not Significant	P < 0.001	P < 0.0001
	7	P < 0.01	P < 0.001	P < 0.0001

(ii)

TREATMENT GROUP	DAY OF CULTURE	NORMOXIA + NAC vs NORMOXIA	HYPOXIA + NAC vs HYPOXIA	NORMOXIA vs HYPOXIA
CTRL + DCF	1	Not Significant	P < 0.01	P < 0.001
	7	Not Significant	P < 0.01	P < 0.05
$NaAsO_2$	1	P < 0.01	P < 0.001	P < 0.0001
	7	P < 0.001	P < 0.001	P < 0.0001
BSO	1	P < 0.05	P < 0.001	P < 0.01
	7	P < 0.05	P < 0.001	P < 0.0001

(iii)

	H9 hESCs		RH1 hESCs	
TREATMENT GROUP AND DAY OF CULTURE	NORMOXIA	HYPOXIA	NORMOXIA	HYPOXIA
$NaAsO_2$ DAY 1	Not Significant	Not Significant	Not Significant	Not Significant
$NaAsO_2$ DAY 7	Not Significant	Not Significant	Not Significant	Not Significant
BSO DAY 1	Not Significant	Not Significant	Not Significant	Not Significant
BSO DAY 7	Not Significant	Not Significant	Not Significant	Not Significant

B (i)

TREATMENT GROUP	NORMOXIA + NAC vs NORMOXIA	HYPOXIA + NAC vs HYPOXIA
Untreated CTRL	Not Significant	Not Significant
$NaAsO_2$	P < 0.01	P < 0.001

(ii)

TREATMENT GROUP	NORMOXIA + NAC vs NORMOXIA	HYPOXIA + NAC vs HYPOXIA
Untreated CTRL	Not Significant	Not Significant
$NaAsO_2$	P < 0.001	P < 0.001

Supplementary Figure 11. Statistical analysis of the effects of antioxidant treatment under normoxia and hypoxia on levels of (A) reactive oxygen species (ROS) and (B) mitochondrial membrane potential (MMP) in (i) H9. (ii) RH1. (iii) H9 and RH1, hESCs.

5

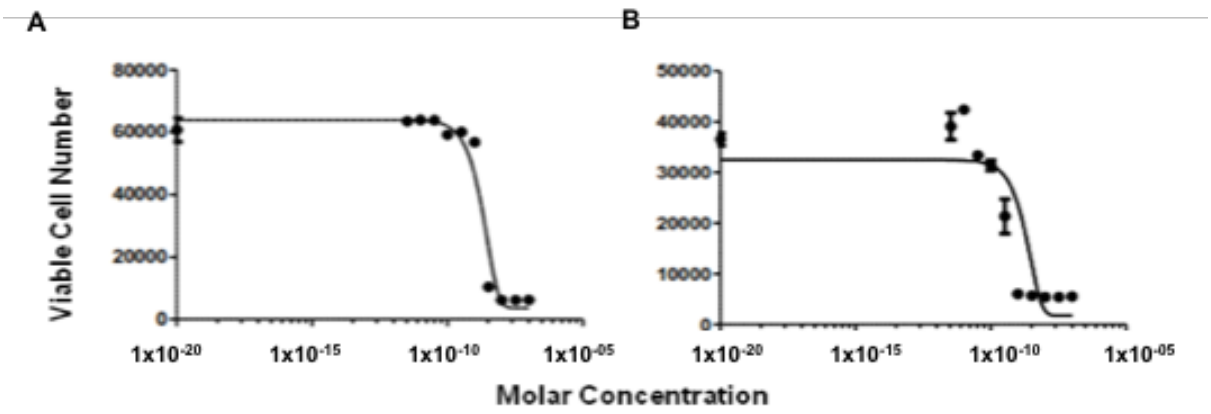

Supplementary Figure 12. Establishment of $NaAsO_2$ concentration treatment cytotoxicity range following continuous exposure of hESCs over seven days.

	Target	Company	Dilution
Primary Antibodies	OCT-3/4	Santa Cruz Biotechnology	1:50
	NANOG	R & D Systems	1:30
	5mC	Active Motif	1:1000
	5hmC	Active Motif	1:1000
Secondary Antibodies	Alexa Fluor® 488 rabbit anti-mouse IgG	Invitrogen	1:200
	Alexa Fluor® 555 donkey anti-goat IgG	Invitrogen	1:200
	Goat anti-rabbit Alexa 555	Invitrogen	1:200
	Goat anti-mouse IgG1 Alexa 488	Invitrogen	1:200

Supplementary Figure 13. Primary and secondary antibodies used in the study, target, source and dilution.

Gene	Reverse Primer	Forward Primer
GAPDH	GGCATGGACTGTGGTCATGAG	TGCACCACCAACTGCTTAGC
β-ACTIN	TTCGTGGATGCCACAGGAC	TACCTCATGAAGATCCTCA
OCT4	GCCTCAAAATCCTCTCGTTG	AGTGAGAGGCAACCTGGAGA
NANOG	ACTGGATGTTCTGGGTCTGG	AACTGGCCGAAGAATAGCAA
SOX2	CTGCCGCCGCCGATGATTGT	AGGGGGAAAGTAGTTTGCTGCCTCT
YAP1	CTGGCCTGTCGGGAGTGGGA	ACCGACCTGGAGGCGCTCTT
KDM4C	TGGCCTGCAGCGATGTATG	CCAGACACTGCCCTAACC
TET1	CAGCTTCTGGGACATTAGCA	GTAAATGGCCCCAAGTCAGA
TET2	TGGTGCCATAAGAGTGGACA	GAGACGCTGAGGAAATACGG
TET3	AACTTGCGAGGTGTCTTGCT	CAGAACGCTGTGATCGTCAT
CDX2	GGTCTATGGCTGTGGGTGGGAG	GAACCTGTGCGAGTGGATGCG
CGα	CTGTGACCCTGTTATATG	CCGCTCCTGATGTGCAGG
PL1	AGTTTGTGTCAAACTTGCTGT	ACACCTACCAGGAGTTTGAAG
BRACHYURY	CCTTGGGCTGCGGCGTCGTACTG	CCCGCGCACTACACACCCCTCACC
BMP2	TCTCGGAAAACCTGAAGCTC	CAGACCACCGGTTGGAGA
VEGF	CTTGCTCTATCTTTCTTTGGTCTGC	AAACCTCACCAAGGCCAGC
GATA2	TGACTTCTCCTGCATGCACT	CCCTAAGCAGCGCAGCAAGAC

Gene	Reverse Primer	Forward Primer
GATA4	TGACTGTCGGCCAAGACCAG	CATCAAGACGGAGCCTGGCC
GATA6	ACGGAGGACGTGACTTCGGC	CCATGACTCCAACTTCCACC
AFP	TCTGCAATGACAGCCTCAAG	TCCCTCCTGCATTCTCTGAT
ALBUMIN	CACGACAGAGTAATCAGGATGCC	GATGAGATGCCTGCTGACTTGC
HNF4α	CAGAGAGGGGCTTGACGAT	AACACAATGCCCACTCACCT
PAX6	TCACTTCCGGGAACTTGAAC	ACCAGCCCTTCGGTGAAT
NESTIN	TGGCACAGGTGTCTCAAGGGTAG	CAGCGTTGGAACAGAGGTTGG
TUBIII	GGCAGTCGCAGTTTTCACAC	GGCCTTTGGACATCTCTTCA
NF-200	ATCTCCTCTGTCTGTTCCTCCA	CTTTCTCCCTTCCAGAAGGACT
HAND1	CGGTGCGTCCTTTAATCCT	CCAAGGATGCACAGTCTGG
GPX1	AATTCCCTCAAGTACGTCCG	CTCGATGTCAATGGTCTGGAA
HO-1	TCACATGGCATAAAGCCCTACAG	ATGGAGCGTCCGCAACCCGACAG
GPX4	AACTACACTCAGCTCGTCG	GCAGGTCCTTCTCTATCACC
SOD1	TGAAGAGAGGCATGTTGGAG	TCTTCATTTCCACCTTTGCC
SOD2	GACAAACCTCAGCCCTAAC	TGCTCCCACACATCAATCC

Supplementary Figure 14. Oligonucleotide primer sequences for genes assessed by RT-PCR.

Supplementary Figure 15. Schematic illustration of the siRNA-mediated knockdown experiments.

Supplementary Figure 16. Episomal plasmids derived for the ectopic expression of epigenetically-marked 2-oxoglutarate-dependent dioxygenases.

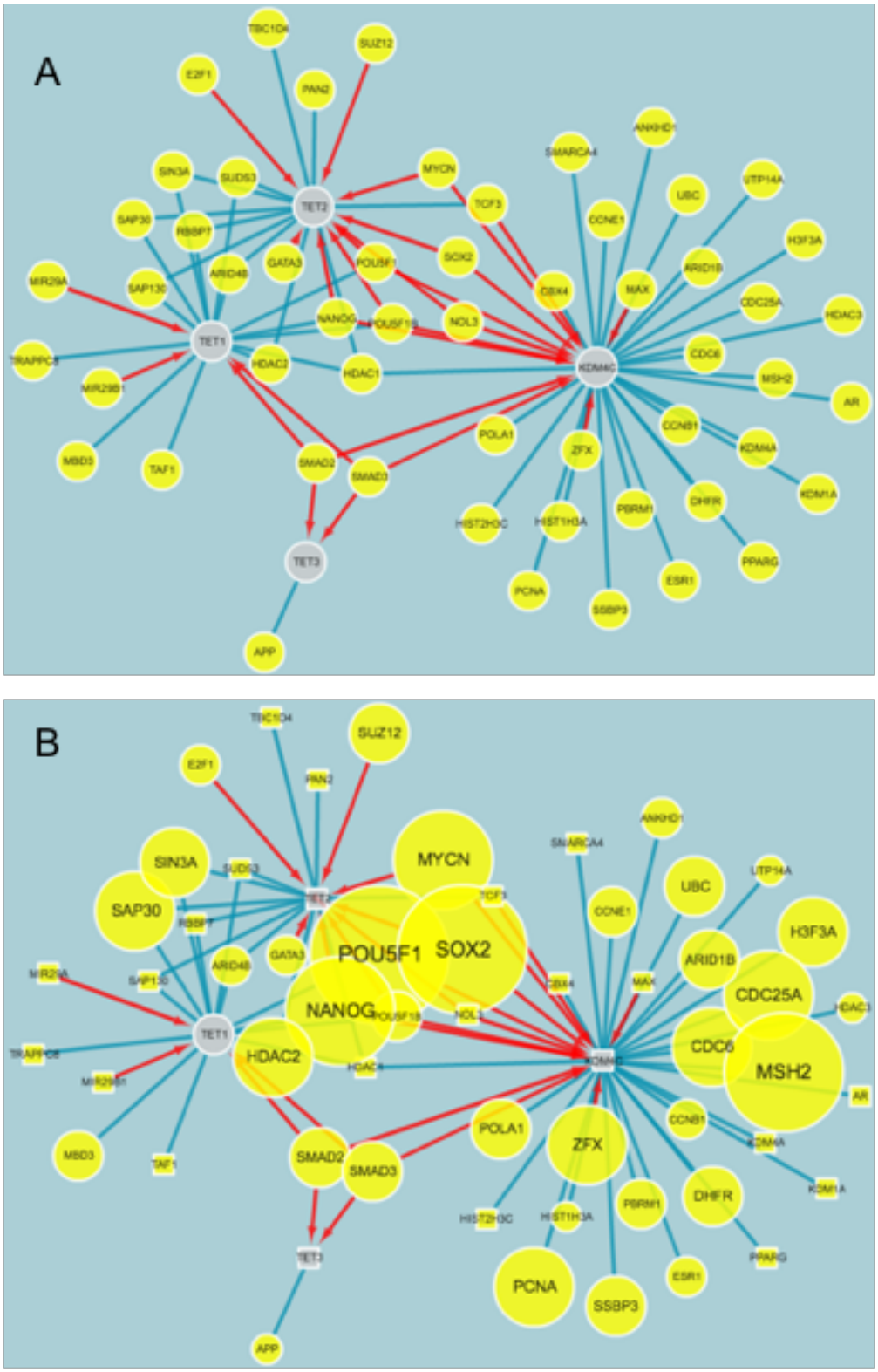

Supplementary Figure 17. StemCellNet network analysis of regulatory and physical interactions with TET1-3 and KDM4C 2-oxoglutarate dioxygenases

References

[1] P.A. De Sousa, R. Steeg, E. Wachter, K. Bruce, J. King, M. Hoeve, S. Khadun, G. McConnachie, J. Holder, A. Kurtz, S. Seltmann, J. Dewender, S. Reimann, G. Stacey, O. O'Shea, C. Chapman, L. Healy, H. Zimmermann, B. Bolton, T. Rawat, I. Atkin, A. Veiga, B. Kuebler, B.M. Serano, T. Saric, J. Hescheler, O. Brustle, M. Peitz, C. Thiele, N. Geijsen, B. Holst, C. Clausen, M. Lako, L. Armstrong, S.K. Gupta, A.J. Kvist, R. Hicks, A. Jonebring, G. Brolen, A. Ebneth, A. Cabrera-Socorro, P. Foerch, M. Geraerts, T.C. Stummann, S. Harmon, C. George, I. Streeter, L. Clarke, H. Parkinson, P.W. Harrison, A. Faulconbridge, L. Cherubin, T. Burdett, C. Trigueros, M.J. Patel, C. Lucas, B. Hardy, R. Predan, J. Dokler, M. Brajnik, O. Keminer, O. Pless, P. Gribbon, C. Claussen, A. Ringwald, B. Kreisel, A. Courtney, T.E. Allsopp, Rapid establishment of the European Bank for induced Pluripotent Stem Cells (EBiSC) - the Hot Start experience, Stem Cell Res, 20 (2017) 105-114.

[2] A. Mohyeldin, T. Garzon-Muvdi, A. Quinones-Hinojosa, Oxygen in stem cell biology: a critical component of the stem cell niche, Cell Stem Cell, 7 (2010) 150-161.

[3] T. Ezashi, P. Das, R.M. Roberts, Low O2 tensions and the prevention of differentiation of hES cells, Proc Natl Acad Sci U S A, 102 (2005) 4783-4788.

[4] N.R. Forsyth, A. Musio, P. Vezzoni, A.H. Simpson, B.S. Noble, J. McWhir, Physiologic oxygen enhances human embryonic stem cell clonal recovery and reduces chromosomal abnormalities, Cloning Stem Cells, 8 (2006) 16-23.

[5] C.E. Forristal, K.L. Wright, N.A. Hanley, R.O. Oreffo, F.D. Houghton, Hypoxia inducible factors regulate pluripotency and proliferation in human embryonic stem cells cultured at reduced oxygen tensions, Reproduction, 139 (2010) 85-97.

[6] S.M. Prasad, M. Czepiel, C. Cetinkaya, K. Smigielska, S.C. Weli, H. Lysdahl, A. Gabrielsen, K. Petersen, N. Ehlers, T. Fink, S.L. Minger, V. Zachar, Continuous hypoxic culturing maintains activation of Notch and allows long-term propagation of human embryonic stem cells without spontaneous differentiation, Cell Prolif, 42 (2009) 63-74.

[7] N.R. Forsyth, A. Kay, K. Hampson, A. Downing, R. Talbot, J. McWhir, Transcriptome alterations due to physiological normoxic (2% O2) culture of human embryonic stem cells, Regenerative medicine, 3 (2008) 817-833.

[8] S.D. Westfall, S. Sachdev, P. Das, L.B. Hearne, M. Hannink, R.M. Roberts, T. Ezashi, Identification of oxygen-sensitive transcriptional programs in human embryonic stem cells, Stem Cells Dev, 17 (2008) 869-881.

[9] E. Narva, J.P. Pursiheimo, A. Laiho, N. Rahkonen, M.R. Emani, M. Viitala, K. Laurila, R. Sahla, R. Lund, H. Lahdesmaki, P. Jaakkola, R. Lahesmaa, Continuous hypoxic culturing of human embryonic stem cells enhances SSEA-3 and MYC levels, PLoS One, 8 (2013) e78847.

[10] D. Kumar, S. Gupta, Y. Yang, N.R. Forsyth, alphaV beta5 and CD44 are oxygen-regulated human embryonic stem cell attachment factors, Biomed Res Int, 2013 (2013) 729281.

[11] Y. Gao, J. Chen, K. Li, T. Wu, B. Huang, W. Liu, X. Kou, Y. Zhang, H. Huang, Y. Jiang, C. Yao, X. Liu, Z. Lu, Z. Xu, L. Kang, J. Chen, H. Wang, T. Cai, S. Gao, Replacement of Oct4 by Tet1 during iPSC induction reveals an important role of DNA methylation and hydroxymethylation in reprogramming, Cell Stem Cell, 12 (2013) 453-469.

[12] S. Pells, E. Koutsouraki, S. Morfopoulou, S. Valencia-Cadavid, S.R. Tomlinson, R. Kalathur, M.E. Futschik, P.A. De Sousa, Novel Human Embryonic Stem Cell Regulators Identified by Conserved and Distinct CpG Island Methylation State, PLoS One, 10 (2015) e0131102.

[13] Y.H. Loh, W. Zhang, X. Chen, J. George, H.H. Ng, Jmjd1a and Jmjd2c histone H3 Lys 9 demethylases regulate self-renewal in embryonic stem cells, Genes & development, 21 (2007) 2545-2557.

[14] Y. Xu, F. Wu, L. Tan, L. Kong, L. Xiong, J. Deng, A.J. Barbera, L. Zheng, H. Zhang, S. Huang, J. Min, T. Nicholson, T. Chen, G. Xu, Y. Shi, K. Zhang, Y.G. Shi, Genome-wide regulation of 5hmC, 5mC, and gene expression by Tet1 hydroxylase in mouse embryonic stem cells, Molecular cell, 42 (2011) 451-464.

[15] H. Wu, A.C. D'Alessio, S. Ito, K. Xia, Z. Wang, K. Cui, K. Zhao, Y.E. Sun, Y. Zhang, Dual functions of Tet1 in transcriptional regulation in mouse embryonic stem cells, Nature, 473 (2011) 389-393.

[16] K. Williams, J. Christensen, M.T. Pedersen, J.V. Johansen, P.A. Cloos, J. Rappsilber, K. Helin, TET1 and hydroxymethylcytosine in transcription and DNA methylation fidelity, Nature, 473 (2011) 343-348.

[17] A. Barchowsky, L.R. Klei, E.J. Dudek, H.M. Swartz, P.E. James, Stimulation of reactive oxygen, but not reactive nitrogen species, in vascular endothelial cells exposed to low levels of arsenite, Free Radic Biol Med, 27 (1999) 1405-1412.

[18] N. Ercal, H. Gurer-Orhan, N. Aykin-Burns, Toxic metals and oxidative stress part I: mechanisms involved in metal-induced oxidative damage, Curr Top Med Chem, 1 (2001) 529-539.

[19] T.K. Hei, M. Filipic, Role of oxidative damage in the genotoxicity of arsenic, Free Radic Biol Med, 37 (2004) 574-581.

[20] M.F. Hughes, Arsenic methylation, oxidative stress and cancer--is there a link?, J Natl Cancer Inst, 101 (2009) 1660-1661.

[21] Y. Wang, Y. Xu, H. Wang, P. Xue, X. Li, B. Li, Q. Zheng, G. Sun, Arsenic induces mitochondria-dependent apoptosis by reactive oxygen species generation rather than glutathione depletion in Chang human hepatocytes, Archives of toxicology, 83 (2009) 899-908.

[22] C. Allegrucci, Y.Z. Wu, A. Thurston, C.N. Denning, H. Priddle, C.L. Mummery, D. Ward-van Oostwaard, P.W. Andrews, M. Stojkovic, N. Smith, T. Parkin, M.E. Jones, G. Warren, L. Yu, R.M. Brena, C. Plass, L.E. Young, Restriction landmark genome scanning identifies culture-induced DNA methylation instability in the human embryonic stem cell epigenome, Hum Mol Genet, 16 (2007) 1253-1268.

[23] K. Amps, P.W. Andrews, G. Anyfantis, L. Armstrong, S. Avery, H. Baharvand, J. Baker, D. Baker, M.B. Munoz, S. Beil, N. Benvenisty, D. Ben-Yosef, J.C. Biancotti, A. Bosman, R.M. Brena, D. Brison, G. Caisander, M.V. Camarasa, J. Chen, E. Chiao, Y.M. Choi, A.B. Choo, D. Collins, A. Colman, J.M. Crook, G.Q. Daley, A. Dalton, P.A. De Sousa, C. Denning, J. Downie, P. Dvorak, K.D. Montgomery, A. Feki, A. Ford, V. Fox, A.M. Fraga, T. Frumkin, L. Ge, P.J. Gokhale, T. Golan-Lev, H. Gourabi, M. Gropp, G. Lu, A. Hampl, K. Harron, L. Healy, W. Herath, F. Holm, O. Hovatta, J. Hyllner, M.S. Inamdar, A.K. Irwanto, T. Ishii, M. Jaconi, Y. Jin, S. Kimber, S. Kiselev, B.B. Knowles, O. Kopper, V. Kukharenko, A. Kuliev, M.A. Lagarkova, P.W. Laird, M. Lako, A.L. Laslett, N. Lavon, D.R. Lee, J.E. Lee, C. Li, L.S. Lim, T.E. Ludwig, Y. Ma, E. Maltby, I. Mateizel, Y. Mayshar, M. Mileikovsky, S.L. Minger, T. Miyazaki, S.Y. Moon, H. Moore, C. Mummery, A. Nagy, N. Nakatsuji, K. Narwani, S.K. Oh, S.K. Oh, C. Olson, T. Otonkoski, F. Pan, I.H. Park, S. Pells, M.F. Pera, L.V. Pereira, O. Qi, G.S. Raj, B. Reubinoff, A. Robins, P. Robson, J. Rossant, G.H. Salekdeh, T.C. Schulz, K. Sermon, J. Sheik Mohamed, H. Shen, E. Sherrer, K. Sidhu, S. Sivarajah, H. Skottman, C. Spits, G.N. Stacey, R. Strehl, N. Strelchenko, H. Suemori, B. Sun, R. Suuronen, K. Takahashi, T. Tuuri, P. Venu, Y. Verlinsky, D. Ward-van Oostwaard, D.J. Weisenberger, Y. Wu, S. Yamanaka, L. Young, Q. Zhou, Screening ethnically diverse human embryonic stem cells identifies a chromosome 20 minimal amplicon conferring growth advantage, Nat Biotechnol, 29 (2011) 1132-1144.

[24] J.A. Thomson, J. Itskovitz-Eldor, S.S. Shapiro, M.A. Waknitz, J.J. Swiergiel, V.S. Marshall, J.M. Jones, Embryonic stem cell lines derived from human blastocysts, Science, 282 (1998) 1145-1147.

[25] J.M. Fletcher, P.M. Ferrier, J.O. Gardner, L. Harkness, S. Dhanjal, P. Serhal, J. Harper, J. Delhanty, D.G. Brownstein, Y.R. Prasad, J. Lebkowski, R. Mandalam, I. Wilmut, P.A. De Sousa, Variations in humanized and defined culture conditions supporting derivation of new human embryonic stem cell lines, Cloning Stem Cells, 8 (2006) 319-334.

[26] A. Ermakov, S. Pells, P. Freile, V.V. Ganeva, J. Wildenhain, M. Bradley, A. Pawson, R. Millar, P.A. De Sousa, A role for intracellular calcium downstream of G-protein signaling in undifferentiated human embryonic stem cell culture, Stem Cell Res, 9 (2012) 171-184.

[27] Y. Masuya, K. Hioki, R. Tokunaga, S. Taketani, Involvement of the tyrosine phosphorylation pathway in induction of human heme oxygenase-1 by hemin, sodium arsenite, and cadmium chloride, J Biochem, 124 (1998) 628-633.

[28] N. Nishioka, K. Inoue, K. Adachi, H. Kiyonari, M. Ota, A. Ralston, N. Yabuta, S. Hirahara, R.O. Stephenson, N. Ogonuki, R. Makita, H. Kurihara, E.M. Morin-Kensicki, H. Nojima, J. Rossant, K. Nakao, H. Niwa, H. Sasaki, The Hippo signaling pathway components Lats and Yap pattern Tead4 activity to distinguish mouse trophectoderm from inner cell mass, Dev Cell, 16 (2009) 398-410.

[29] M. Liu, S. Zhao, Q. Lin, X.P. Wang, YAP regulates the expression of Hoxa1 and Hoxc13 in mouse and human oral and skin epithelial tissues, Mol Cell Biol, 35 (2015) 1449-1461.

[30] R. Martinez-Zamudio, H.C. Ha, Environmental epigenetics in metal exposure, Epigenetics, 6 (2011) 820-827.

[31] J.F. Reichard, M. Schnekenburger, A. Puga, Long term low-dose arsenic exposure induces loss of DNA methylation, Biochemical and biophysical research communications, 352 (2007) 188-192.

[32] E. Dopp, L.M. Hartmann, U. von Recklinghausen, A.M. Florea, S. Rabieh, U. Zimmermann, B. Shokouhi, S. Yadav, A.V. Hirner, A.W. Rettenmeier, Forced uptake of trivalent and pentavalent methylated and inorganic arsenic and its cyto-/genotoxicity in fibroblasts and hepatoma cells, Toxicol Sci, 87 (2005) 46-56.

[33] V. Zachar, S.M. Prasad, S.C. Weli, A. Gabrielsen, K. Petersen, M.B. Petersen, T. Fink, The effect of human embryonic stem cells (hESCs) long-term normoxic and hypoxic cultures on the maintenance of pluripotency, In Vitro Cell Dev Biol Anim, 46 (2010) 276-283.

[34] J. Mathieu, Z. Zhang, A. Nelson, D.A. Lamba, T.A. Reh, C. Ware, H. Ruohola-Baker, Hypoxia induces re-entry of committed cells into pluripotency, Stem Cells, 31 (2013) 1737-1748.

[35] T. Wang, K. Chen, X. Zeng, J. Yang, Y. Wu, X. Shi, B. Qin, L. Zeng, M.A. Esteban, G. Pan, D. Pei, The histone demethylases Jhdm1a/1b enhance somatic cell reprogramming in a vitamin-C-dependent manner, Cell Stem Cell, 9 (2011) 575-587.

[36] S. Ito, A.C. D'Alessio, O.V. Taranova, K. Hong, L.C. Sowers, Y. Zhang, Role of Tet proteins in 5mC to 5hmC conversion, ES-cell self-renewal and inner cell mass specification, Nature, 466 (2010) 1129-1133.

[37] J.M. Freudenberg, S. Ghosh, B.L. Lackford, S. Yellaboina, X. Zheng, R. Li, S. Cuddapah, P.A. Wade, G. Hu, R. Jothi, Acute depletion of Tet1-dependent 5-hydroxymethylcytosine levels impairs LIF/Stat3 signaling and results in loss of embryonic stem cell identity, Nucleic Acids Res, 40 (2012) 3364-3377.

[38] Y. Katoh, M. Katoh, Comparative integromics on JMJD2A, JMJD2B and JMJD2C: preferential expression of JMJD2C in undifferentiated ES cells, Int J Mol Med, 20 (2007) 269-273.

[39] S. Beyer, M.M. Kristensen, K.S. Jensen, J.V. Johansen, P. Staller, The histone demethylases JMJD1A and JMJD2B are transcriptional targets of hypoxia-inducible factor HIF, The Journal of biological chemistry, 283 (2008) 36542-36552.

[40] P.J. Pollard, C. Loenarz, D.R. Mole, M.A. McDonough, J.M. Gleadle, C.J. Schofield, P.J. Ratcliffe, Regulation of Jumonji-domain-containing histone demethylases by hypoxia-inducible factor (HIF)-1alpha, Biochem J, 416 (2008) 387-394.

[41] S. Wellmann, M. Bettkober, A. Zelmer, K. Seeger, M. Faigle, H.K. Eltzschig, C. Buhrer, Hypoxia upregulates the histone demethylase JMJD1A via HIF-1, Biochemical and biophysical research communications, 372 (2008) 892-897.

[42] X. Xia, M.E. Lemieux, W. Li, J.S. Carroll, M. Brown, X.S. Liu, A.L. Kung, Integrative analysis of HIF binding and transactivation reveals its role in maintaining histone methylation homeostasis, Proc Natl Acad Sci U S A, 106 (2009) 4260-4265.

[43] J. Yang, I. Ledaki, H. Turley, K.C. Gatter, J.C. Montero, J.L. Li, A.L. Harris, Role of hypoxia-inducible factors in epigenetic regulation via histone demethylases, Ann N Y Acad Sci, 1177 (2009) 185-197.

[44] W. Luo, R. Chang, J. Zhong, A. Pandey, G.L. Semenza, Histone demethylase JMJD2C is a coactivator for hypoxia-inducible factor 1 that is required for breast cancer progression, Proc Natl Acad Sci U S A, 109 (2012) E3367-3376.

[45] C.J. Mariani, A. Vasanthakumar, J. Madzo, A. Yesilkanal, T. Bhagat, Y. Yu, S. Bhattacharyya, R.H. Wenger, S.L. Cohn, J. Nanduri, A. Verma, N.R. Prabhakar, L.A. Godley, TET1-mediated hydroxymethylation facilitates hypoxic gene induction in neuroblastoma, Cell Rep, 7 (2014) 1343-1352.

[46] Y.P. Tsai, H.F. Chen, S.Y. Chen, W.C. Cheng, H.W. Wang, Z.J. Shen, C. Song, S.C. Teng, C. He, K.J. Wu, TET1 regulates hypoxia-induced epithelial-mesenchymal transition by acting as a co-activator, Genome biology, 15 (2014) 513.

[47] W.L. Berry, R. Janknecht, KDM4/JMJD2 histone demethylases: epigenetic regulators in cancer cells, Cancer research, 73 (2013) 2936-2942.

[48] R. Petruzzelli, D.R. Christensen, K.L. Parry, T. Sanchez-Elsner, F.D. Houghton, HIF-2alpha regulates NANOG expression in human embryonic stem cells following hypoxia and reoxygenation through the interaction with an Oct-Sox cis regulatory element, PLoS One, 9 (2014) e108309.

[49] J.P. Pinto, R.K. Reddy Kalathur, R.S. Machado, J.M. Xavier, J. Braganca, M.E. Futschik, StemCellNet: an interactive platform for network-oriented investigations in stem cell biology, Nucleic Acids Res, 42 (2014) W154-160.

[50] Y. Costa, J. Ding, T.W. Theunissen, F. Faiola, T.A. Hore, P.V. Shliaha, M. Fidalgo, A. Saunders, M. Lawrence, S. Dietmann, S. Das, D.N. Levasseur, Z. Li, M. Xu, W. Reik, J.C. Silva, J. Wang, NANOG-dependent function of TET1 and TET2 in establishment of pluripotency, Nature, 495 (2013) 370-374.

[51] K.P. Koh, A. Yabuuchi, S. Rao, Y. Huang, K. Cunniff, J. Nardone, A. Laiho, M. Tahiliani, C.A. Sommer, G. Mostoslavsky, R. Lahesmaa, S.H. Orkin, S.J. Rodig, G.Q. Daley, A. Rao, Tet1 and Tet2 regulate 5-hydroxymethylcytosine production and cell lineage specification in mouse embryonic stem cells, Cell Stem Cell, 8 (2011) 200-213.

[52] M.M. Dawlaty, K. Ganz, B.E. Powell, Y.C. Hu, S. Markoulaki, A.W. Cheng, Q. Gao, J. Kim, S.W. Choi, D.C. Page, R. Jaenisch, Tet1 is dispensable for maintaining pluripotency and its loss is compatible with embryonic and postnatal development, Cell Stem Cell, 9 (2011) 166-175.

[53] T.R. Durham, E.T. Snow, Metal ions and carcinogenesis, EXS, (2006) 97-130.

[54] G.M. Hong, L.J. Bain, Arsenic exposure inhibits myogenesis and neurogenesis in P19 stem cells through repression of the beta-catenin signaling pathway, Toxicol Sci, 129 (2012) 146-156.

[55] V.N. Ivanov, T.K. Hei, Induction of apoptotic death and retardation of neuronal differentiation of human neural stem cells by sodium arsenite treatment, Exp Cell Res, 319 (2013) 875-887.

[56] V.N. Ivanov, G. Wen, T.K. Hei, Sodium arsenite exposure inhibits AKT and Stat3 activation, suppresses self-renewal and induces apoptotic death of embryonic stem cells, Apoptosis, 18 (2013) 188-200.

[57] T. Burdon, A. Smith, P. Savatier, Signalling, cell cycle and pluripotency in embryonic stem cells, Trends Cell Biol, 12 (2002) 432-438.

[58] L. Armstrong, O. Hughes, S. Yung, L. Hyslop, R. Stewart, I. Wappler, H. Peters, T. Walter, P. Stojkovic, J. Evans, M. Stojkovic, M. Lako, The role of PI3K/AKT, MAPK/ERK and NFkappabeta signalling in the maintenance of human embryonic stem cell pluripotency and viability highlighted by transcriptional profiling and functional analysis, Hum Mol Genet, 15 (2006) 1894-1913.

[59] A.R. Ji, S.Y. Ku, M.S. Cho, Y.Y. Kim, Y.J. Kim, S.K. Oh, S.H. Kim, S.Y. Moon, Y.M. Choi, Reactive oxygen species enhance differentiation of human embryonic stem cells into mesendodermal lineage, Exp Mol Med, 42 (2010) 175-186.

[60] C. Batandier, E. Fontaine, C. Keriel, X.M. Leverve, Determination of mitochondrial reactive oxygen species: methodological aspects, J Cell Mol Med, 6 (2002) 175-187.

[61] M. Karlsson, T. Kurz, U.T. Brunk, S.E. Nilsson, C.I. Frennesson, What does the commonly used DCF test for oxidative stress really show?, Biochem J, 428 (2010) 183-190.

[62] G.H. Danet, Y. Pan, J.L. Luongo, D.A. Bonnet, M.C. Simon, Expansion of human SCID-repopulating cells under hypoxic conditions, J Clin Invest, 112 (2003) 126-135.

[63] C. Piccoli, A. D'Aprile, M. Ripoli, R. Scrima, L. Lecce, D. Boffoli, A. Tabilio, N. Capitanio, Bone-marrow derived hematopoietic stem/progenitor cells express multiple isoforms of NADPH oxidase and produce constitutively reactive oxygen species, Biochemical and biophysical research communications, 353 (2007) 965-972.

[64] N.Y. Chia, Y.S. Chan, B. Feng, X. Lu, Y.L. Orlov, D. Moreau, P. Kumar, L. Yang, J. Jiang, M.S. Lau, M. Huss, B.S. Soh, P. Kraus, P. Li, T. Lufkin, B. Lim, N.D. Clarke, F. Bard, H.H. Ng, A genome-wide RNAi screen reveals determinants of human embryonic stem cell identity, Nature, 468 (2010) 316-320.

[65] M.C. Ryan, B.R. Zeeberg, N.J. Caplen, J.A. Cleland, A.B. Kahn, H. Liu, J.N. Weinstein, SpliceCenter: a suite of web-based bioinformatic applications for

evaluating the impact of alternative splicing on RT-PCR, RNAi, microarray, and peptide-based studies, BMC Bioinformatics, 9 (2008) 313.

5